The Pennsylvania State University

The Graduate School

PREDICTION OF GEOTECHNICAL PROPERTIES OF COAL SLURRIES USING CONE PENETRATION TEST

A Thesis in

Civil Engineering

by

Rong Zhao

Submitted in Partial Fulfillment
of the Requirements
for the Degree of

Master of Science

May 2019

The thesis of Rong Zhao was reviewed and approved* by the following:

Ming Xiao
Associate Professor of Civil Engineering
Thesis Advisor

Tong Qiu
Associate Professor of Civil Engineering

Shimin Liu
Associate Professor of Earth and Mineral Engineering

Patrick J. Fox
Department Head of Civil and Environmental Engineering

*Signatures are on file in the Graduate School

ABSTRACT

This thesis presents an experimental research for studying liquefaction potential of coal slurry under seismic motions by cone penetration test and correlations of coal slurry physical and dynamic properties such as shear modulus, pre-consolidation stress, and soil classification. Total of eight cone penetration tests are performed, six before simulated earthquake shaking and two after shaking. Tip resistance, sleeve friction and pore pressure of coal slurry are collected during CPT and used to analyze coal slurry. Friction ratio, as one of the basic parameters of coal slurry, is calculated directly from tip and sleeve resistance. The ratio of cyclic resistance ratio and cyclic stress ratio is used to evaluate liquefaction potential of coal slurry. CPT at different locations in laminar shear box yield varying cyclic resistance ratio based on the tip resistance.

Three soil properties of coal slurry are correlated with CPT as the main findings of this research. Shear modulus and shear wave velocity of dried coal slurry are measured from resonant column test and compared with shear modulus correlated from CPT. Pre-consolidation stress of coal slurry is measured from oedometer test of in-situ undisturbed coal slurry samples and compared to the correlated pre-consolidation stress derived from CPT. Soil classification is determined by lab testing such as sieve analysis, hydrometer test, and Atterberg limit test and also compared to the correlated soil classification from CPT.

The coal slurry is anticipated to liquefy with an arbitrary ground acceleration estimated based on cyclic resistance ratio. The shear modulus of coal slurry measured from resonant column test is less than correlated shear modulus from CPT results, but in an

acceptable range. The correlated pre-consolidation stress from CPT is close to the pre-consolidation stress measured from oedometer test. The correlated soil classification from CPT also agrees with the classification based on laboratory testing.

TABLE OF CONTENTS

LIST OF FIGURES

LIST OF TABLES

ACKNOWLEDGEMENTS

This research requires a continued work and intensive labor from the research group and would not have been possible without all of their effort. I would like to thank my advisor Dr. Ming Xiao for his support and guidance throughout my study. My graduate study is a precious experience with his mentorship where I learn more than just the materials of geotechnical engineering.

I would like to thank Dan Fura for his great help in every aspect in the Civil Infrastructure Testing and Evaluation Laboratory (CITEL). His help and support with the laboratory equipment and ideas are very important to my research. I would also like to thank Dr. Tong Qiu for his advice and generous support with the resonant column testing. Special thanks to Dr. Shimin Liu for serving on my thesis committee and providing advice and review of the thesis.

Thanks are due to my fellow research team members, Sajjad Salam, Yen-Chieh Wang, Jintai Wang, and Min Liew, for their immense help and advice in the field and laboratory testing. I am grateful to my mother (Yang Li) and father (Jianliang Zhao) for their unconditional love and support.

CHAPTER 1 INTRODUCTION

1.1 Problem Statement and Research Motivation

Tailings dam failure is one of the most catastrophic events in the world. A catastrophic release of tailings can lead to long-term environmental damage with significant cleanup costs (Chambers, 2015). Mining industries yield significant amount of tailings after washing the minerals each year. These wastes are usually stored in an impoundment built near the mining site. However, many coal mining sites are surrounded by villages and rivers. Failure of the tailings dam can discharge toxic wastes to the nearby villages and rivers, causing irreversible damage to the communities and environment. Soil liquefaction is one of the most common reasons that cause failure of tailings dams. It is triggered by the seismic motions such as earthquakes or blasting. Soil liquefaction happens when the vertical effective stress on the soil decreases to zero by the increased pore pressure. This makes soil particles free to move and results in increased lateral earth pressure on the tailings dam and could potentially cause tailings dam failure.

There are more than 1300 mine tailings impoundments in the United States that allow the mining and processing of coal and other minerals, and over 200 of them are classified as having high hazards potential by the Federal Emergency Management Agency's hazard rating system (FEMA, 2019). A corpus of 147 cases of worldwide tailing dam disasters is compiled in a database and fifteen percent of them is caused by seismic liquefaction (Rico, 2007). There are 17 tailings dam failures since 1980 where the volume of the waste released is significant (WISE, 2019). For example, the Kingston fossil plant

coal fly ash slurry spill released 4-million m^3 waste in 2008 (Tetra Tech EM, 2009). The released coal slurry composes heavy metals, which can cause ecological and environmental hazards in rivers and lakes, and pollute nearby villages. In 2014, Mount Polley tailings dam failure (Figure 1-1) happened in the British Columbia, Canada. According to the government-ordered report, 24 million cubic meters of silt and water had flooded to Polley lake and continued to nearby Quesnel lake and Cariboo river. The negative environmental impact caused by the overflow of mining waste is substantial. It takes years even decades to recover from the damage with billions of dollars spent and huge amount of efforts (Marshall, 2018). A recent tailings dam failure occurred in Brazil on Nov 5, 2015 known as the Fundão Tailings Dam failure as shown in Figure 1-2. Eighty percent of its stored waste had been released and 19 people were killed. Buffalo Creek flood and disaster resulted in 125 fatalities and 4000 people homeless (Davies et al. 1972). Another collapse of a Brazilian dam controlled by miner Vale happened in the end of January 2019, with 110 people confirmed dead and another 238 missing (Stargardter, 2019).

(a) B.C.'s Mount Polley, waste flow into lake (b) B.C.'s Mount Polley, breakage of wall

Figure 1-1. Examples of tailings dam failures: B.C.'s Mount Polley tailings dam failure, photo courtesy of Marshall 2018

(a) before dam failure (b) after dam failure

Figure 1-2. Examples of tailings dam failures: Fundão Tailings Dam failure, photo by Fundão Tailings Dam Review Panel.

To ensure the stability of coal slurry impoundment, in-situ testing of soil properties becomes especially important. This research aims at finding the liquefaction potential using cone penetration test and correlating the analyzed data to soil properties. Research on tailings dam structure and properties of waste coal slurry is a significant step to prevent any environmental and economical disasters caused by tailing dam failure. Using in-situ methods such as cone penetration test is highly efficient in time and cost. It also reduces the inaccuracy of results caused by disturbance of soil samples. Furthermore, correlations between the CPT results and certain soil properties can be established for advanced stability analysis of the impoundment.

1.2 Research Objectives

The first objective of this research is to analyze the occurrence of liquefaction of coal slurry by performing cone penetration tests after shake table testing. The second objective is to correlate the tip and sleeve resistance from CPT data with coal slurry properties such as shear modulus, pre-consolidation stress, and soil classification for future reference if in-situ data are available. A laminar shear box on the shake table is used to deposit coal slurry and simulate earthquake motion. Acceleration of soil particles and pore pressure built up in the coal slurry during the simulated motion are recorded and used for liquefaction analysis.

1.3 Thesis Outline

This thesis consists of five chapters. Introduction of the research is given in chapter 1. Literature review of coal slurry impoundments, field testing methods of soil, liquefaction potential of coal slurry, correlations between CPT results with pre-consolidation stress, shear modulus, and soil classification are presented in chapter 2. Chapter 3 presents the methodology of calculating the liquefaction potential of coal slurry using CPT data and the analysis of the results. Chapter 4 elaborates three correlations that can be made based on the CPT data. Chapter 5 presents the summary and conclusions derived from this study with recommendations of future work.

CHAPTER 2 LITERATURE REVIEW

2.1 Tailings Dams of Coal Slurry

2.1.1 Tailings Dam Construction Types

Tailings dams are used to store waste from processing the minerals from impurities. There are three types of tailing dams as shown in Figure 2-1. Tailings dams are different in dam-life design and dam-construction design compared to regular water reservoirs. As a tailings dam must be designed to safely impound the waste without the option of draining the waste, it requires additional considerations in regard to the seismic and hydrologic events that the dam might experience. Liquefaction of tailings due to a large seismic event can lead to large tailings release through a ruptured dam.

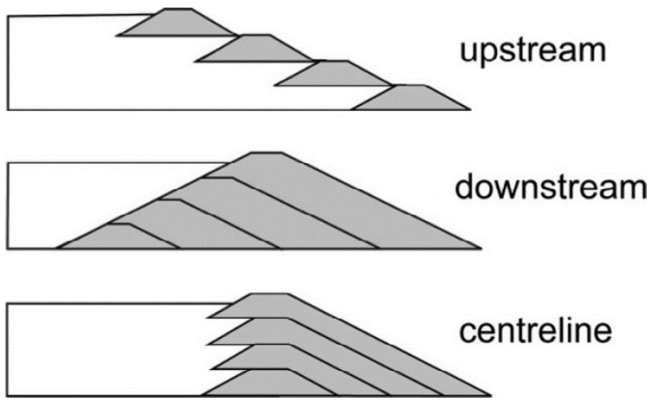

Figure. 2-1. Schematic illustrations of upstream, downstream and centerline sequentially raised tailings dams (Vick, 1983)

The construction of tailings dam can be either (1) upstream, (2) downstream, or (3) centerline. Downstream construction is the safest type of construction. However, it also

has the highest cost among the three choices. Upstream construction is the least secure because it relies on the stability of the tailings themselves as a foundation of dam construction (Davies, 2002). The construction of upstream dams often uses the coarse material from tailings. This saturated and unconsolidated material is susceptible to liquefaction under seismic loading. Centerline construction is a hybrid of the previous two dam construction, and from a seismic stability standpoint the risk of failure lies between them. “Selection of the embankment type must be based on the specific characteristics of each mine, mill, tailings grind, climate, seismicity topography and other factors” (Watson et al., 2010).

2.1.2 Tailings Properties and Impoundment

Tailings are a generic term as it describes the by-product of aluminum, coal, oil sands, uranium and precious metals in their extraction industries. Their particles are commonly angular to very angular, and this morphology imposes a high friction angle on dry tailings (Mulligan, 1996; Sarsby, 2000; Bjelkevik, 2005). Tailings grain size is highly variable and difficult to generalize. Sarsby (2000) defined hard rock tailings particle sizes as largely gravel-free and clay-free, with sand being more common than silt. However, clay particles are found very common in coal slurry. A generalized range of tailings bulk density is 1.8 – 1.9 t/m^3 with a specific gravity of 2.6 – 2.8 (Sarsby, 2000; Bjelkevic, 2005). The coal slurry in this research is found with a smaller specific gravity around 2.1 – 2.3. Coal slurry is mainly composed of water, coal, sand, and clay. However, it also contains carcinogenic chemicals used to process coal and toxic heavy metals that are present in coal

(Ducatman, 2010). This research specifically focuses on the by-product from coal mining. Figure 2-2 shows tailings from Jeddo coal mining's impoundment in eastern Pennsylvania. After the tailings being transported to the impoundment, it settles down and the water table is normally near the soil surface.

(a) In-situ coal slurry and water level (b) Tailing site

Figure 2-2. Examples of tailings and impoundment: (a) Tailings from coal mining in Jeddo site; (b) Tailing impoundment, Pennsylvania. Photos taken in October 2018.

The significant amount and often hazardous nature of the material held within tailings dams means that their failure, and the ensuing discharge into river systems, will invariably affect water and sediment quality, and aquatic and human life for potentially hundreds of kilometers downstream (Edwards, 1996; Macklin et al., 2006). Tailings dam failure caused significant damage to environment and economics in the past (WISE, 2012). For example, a major dike failure occurred on the north slopes of the ash pond at the Tennessee Valley Authority (TVA)'s Kingston Fossil Plant. This failure resulted in the

release of approximately 5.4 million cubic yards of coal ash spilling onto adjacent land and into the Emory River. While there was no loss of life, 26 homes were either destroyed or damaged. TVA estimated the cost of this spill to be between $675 million and $975 million, not including potential litigation and claims, community recovery support, environmental remediation and long-term monitoring (Kilgore, 2009). Another mining dam in Brazil collapsed and buried more than 150 people in January, 2019 (Darlington et al, 2019). The tailings dam was built in upstream to hold waste from washing the iron ore. Areas where the dam appears to have collapsed first are shown below in Figure 2-3.

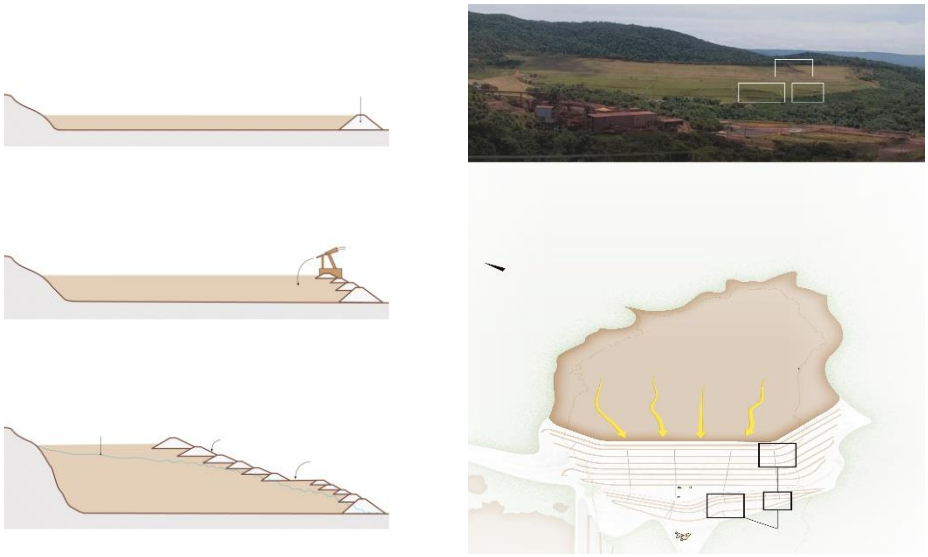

(a) (b)

Figure 2-3. (a) Upstream construction of failed tailing dams in Brumadinho, Brazil (b) Area where the dam appears to collapse.

2.2 Field Testing Methods of Soil

There are two general approaches for evaluating liquefaction potential of a deposited saturated sand or other soils subjected to earthquake. The first method is based on field observations of the performance of soil deposits in previous earthquakes; this approach involves the consideration of soil in-situ characteristic from the deposits to determine similarities between old sites and new sites (Seed et al, 1983). The second approach is based on an evaluation of the cyclic stress ratio or strain conditions by a proposed design earthquake with a calculated liquefaction factor of safety. The comparison is made to the representative samples of the deposit where liquefaction is observed. This method provides an adequate simulation of field conditions and results permitting an assessment of the soil behavior under field conditions (Seed et al, 1983). There are four in situ test methods widely used in the simplified procedures to determine the liquefaction potential including (1) the standard penetration test (SPT); (2) the cone penetration test (CPT); (3) measurement of in situ shear wave velocity v_s; and (4) the Becker penetration test (BPT). Each of them has advantages and disadvantages for evaluating liquefaction resistance in the field such as liquefaction available data, stress-strain behavior, repeatability, and soil type.

In the assessment of coal slurry's properties, it is difficult to obtain results by directly using in situ tests due to its softness and site accessibility. Therefore, building a correlation between in situ data and soil properties is becoming an efficient way to evaluate its liquefaction potential. Many in situ tests have switched from SPT to CPT due to the advantage of the latter one: CPT can provide in situ data much more rapidly with less cost

and the continuous record of penetration, it provides a better subsurface topography, and analysis based on its results has been vastly applied during the past 20 years. Conversion between tip resistance from CPT and blow counts from SPT is well established for clean sands and silty sands (Schmertmann, 1979).

2.3 Coal Slurry Liquefaction Potential

One of the first attempt to explain the liquefaction phenomenon in sandy soils was made by Casagrande (1936) and is based on the concept of critical void ratio (Das, 2015). Soil liquefaction causes loss of strength in soil and results hazards such as dam failure, landslides, and settlement of structures. It is mostly associated with medium to fine grained saturated cohesionless soils. The definition of soil liquefaction is when a soil element reaches the condition of essentially zero effective stress, the soil has very little stiffness and large deformation can occur during cyclic loading (Robertson and Wride, 1997). Normally, sand deposit decreases in volume when it has a void ratio larger than the critical void ratio by vibration during a seismic event. However, it is assumed the soil has free drainage. In an earthquake, since the drainage is unable to occur during the vibration within such a short time interval, the pore pressure builds up and eventually equals to the effective stress. Under this condition, the soil does not have any shear strength and can be easily deformed.

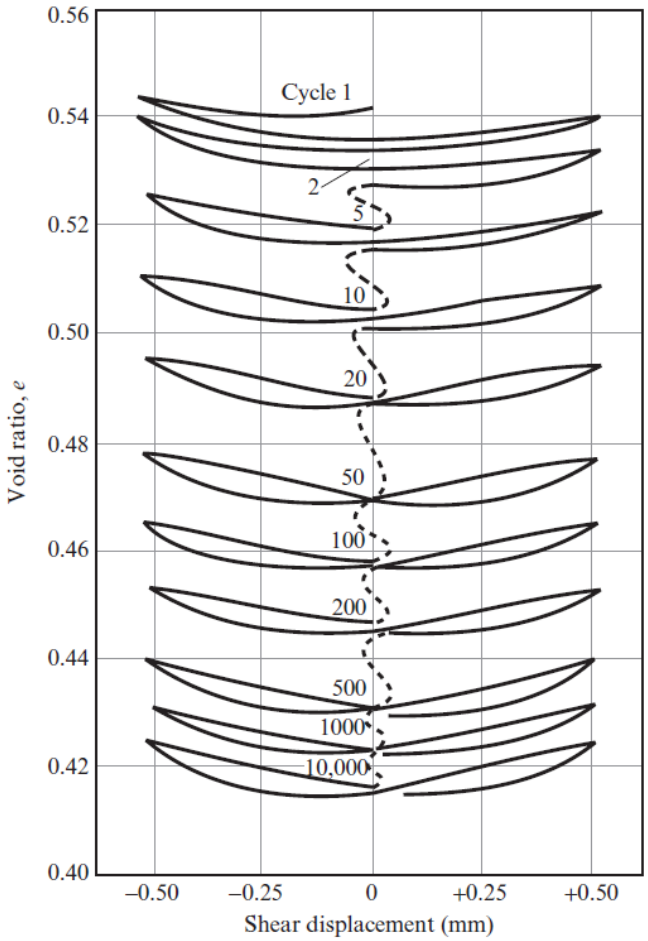

Figure 2-4. Void ratio versus cyclic shear displacement for densification of a sand with successive cycles of shear (from Youd, 1972)

Figure 2-4 above shows the gradual densification of sand by repeated back-and-forth straining in a simple shear test. The liquefaction potential decreases with smaller void ratio by densification of soil. Thus, the aging of soil decreases the potential of liquefaction. There is no limit of drainage in this case. The void ratio of soil reduces fast in the first several cycles and the rate of void ratio reduction becomes smaller as the sand becomes

more densified. The decrease of volume in sand can only occur when there is free drainage. Under earthquake conditions, there is no drainage allowed due to rapid cyclic straining.

The simplified procedure proposed by Seed and Idriss (1971) is the most widely used method for liquefaction potential evaluation. The factor of safety against liquefaction is defined as the ratio of CRR over CSR:

$$Fs = \frac{CRR}{CSR} \tag{2-1}$$

Cyclic stress ratio (CSR) represents the seismic loading on soil, and cyclic resistance ratio (CRR) represents the capacity of the soil to resist liquefaction. The simplified procedure necessitates the use of in situ index testing in common practice where liquefaction is likely to occur if Fs < 1.0 (Das, 2015).

2.4 Review of Correlation Between Pre-Consolidation Stress and CPT

The determination of pre-consolidation stress of a soil is primarily based on the oedometer test in the lab. For many types of soils, sample collection can be challenging especially when high quality, undisturbed soil samples are required to obtain accurate soil parameters from lab testing, such as pre-consolidation stress. However, with in-situ cone penetration test including pore pressure measurement, the inaccuracy of experimental results can be minimized.

The pre-consolidation pressure σ'_c can be approximated from the expression by Senneset et al. (1985) when pore pressure is measured with a cone penetration test:

$$\sigma_c' + a = \frac{q_T' + a}{N_{qc}} \tag{2-2}$$

where q'_T is the effective cone resistance, a is the attraction over a stress range $\Delta\sigma'$ defined by the Mohr-Coulomb failure criterion in Figure 2-5 below, and N_{qc} is a bearing coefficient defined by equation 2-3.

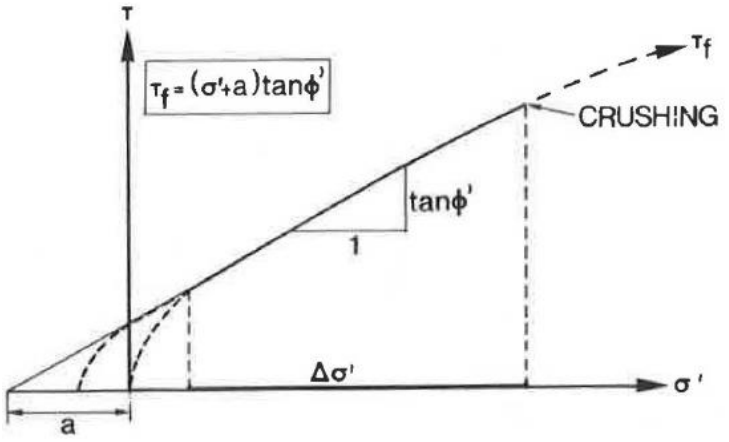

Figure 2-5 Definition of strength parameter in the Mohr-Coulomb criterion (Senneset, 1985)

$$N_{qc} = \frac{N_q + N_u B_q}{1 + N_u B_q} \tag{2-3}$$

The hatched area in Figure 2-6 reflects the variation in the product $N_u B_q$ when the Prandtl solution for N_{qc} the bearing capacity coefficient is used. In this approach, it is assumed that the pre-consolidation stress (σ'_c), the excess pore pressure around the cone (Δu_T), and the effective shear strength parameters such as attraction (a) and tangent of effective friction angle ($tan\phi'$) determine the effective cone resistance (q'_T).

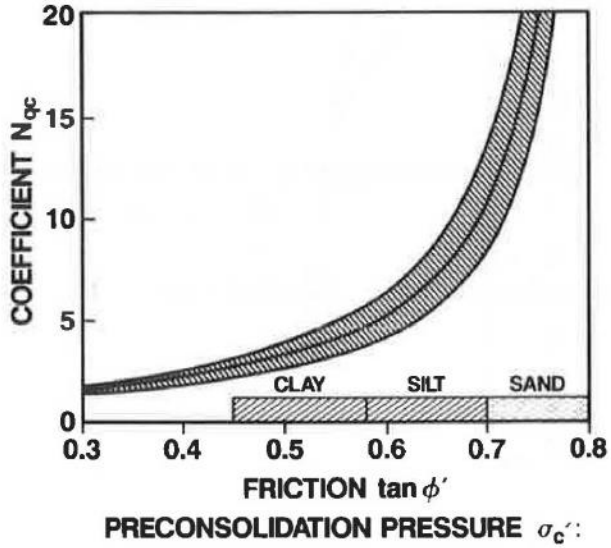

Figure 2-6 Bearing capacity coefficient N_{qc} for interpretation of pre-consolidation pressure σ'_c (Senneset et al., 1985)

2.5 Review of Correlation Between Shear Wave Velocity and CPT Testing

Correlation of shear modulus and cone penetration resistance has been discussed and further developed by Rix and Stokoe (1991). The direct correlation between G_{max} and q_c cannot be established without uncertainty since factors such as fines content, particle angularity, and particle mineralogy. A modified correlation is presented by Rix and Stokoe (1991) for mortar sand where two properties could be correlated both in Figure 2-8 and by an empirical equation specifically for washed mortar sand. Correlations proposed by Baldi et al. (1985) for washed mortar sand data are compared in that research; the cone tip resistances and initial shear modulus were independently measured by US Geological Survey with crosshole tests and cone penetration tests. A comparison of Heber road data

with correlation proposed by Baldi et al. (1985) is made in Figure 2-7 and included in further correlation.

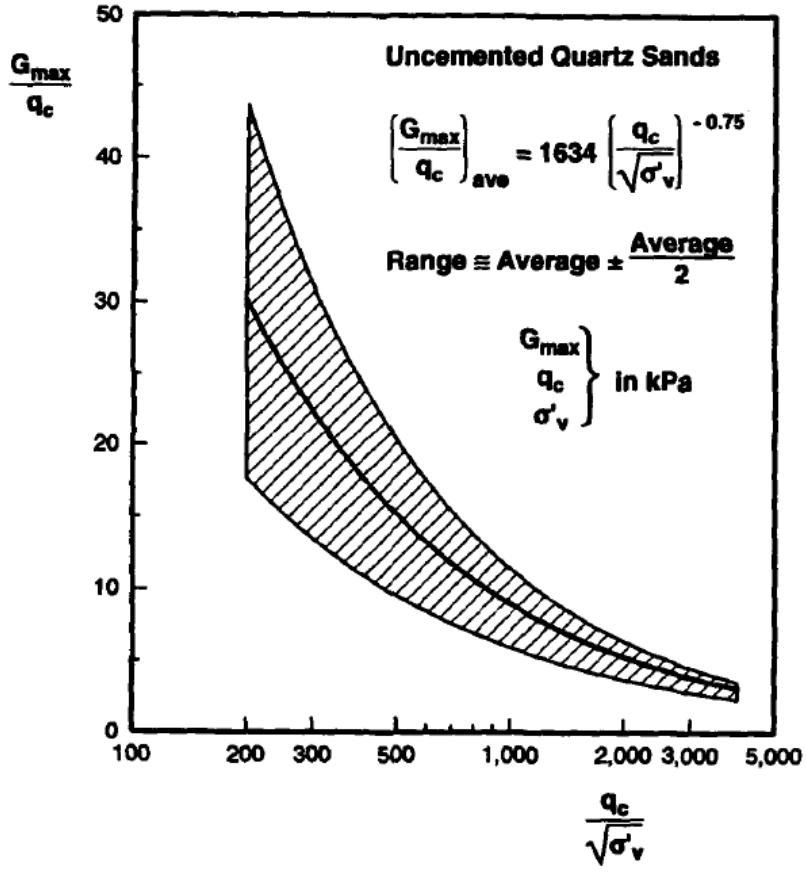

Figure 2-7 Proposed Modified Correlation Between G_{max} and q_c for uncemented, Quartz sands showing average and range in values Baldi et al. (1985).

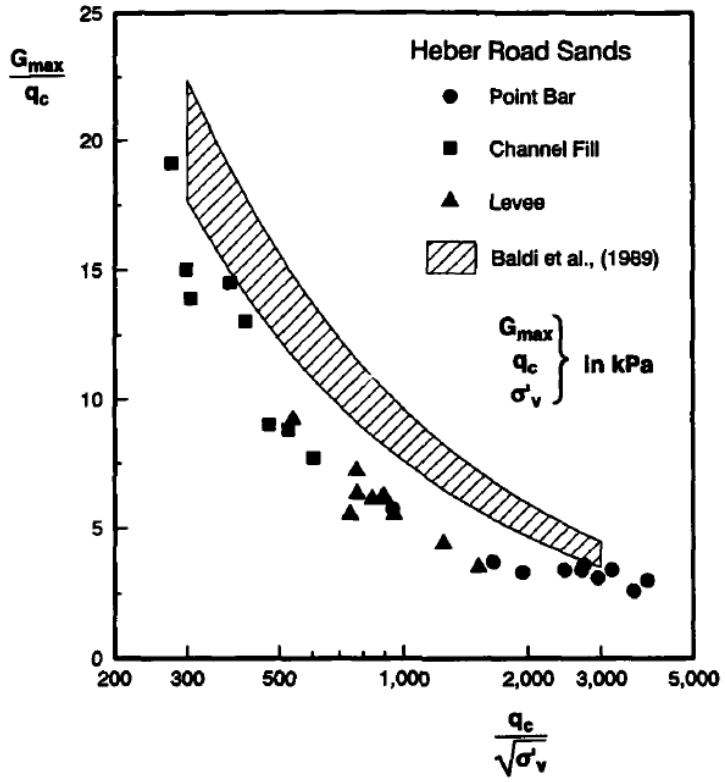

Figure 2-8 Comparison of Heber Road Data with correlation proposed by Baldi et al. (1985)

2.6 Review of Correlation Between Soil Classification and CPT

One of the most comprehensive work of correlation between cone penetration data and unified soil classification system (USCS) is developed by Douglas and Olsen (1981). The soil classification chart is shown in Figure. 2-9. The correlation is based on extensive data collected from areas in California, Oklahoma, Utah, Arizona, and Nevada (USGS, 1980). Figure 2-9 is a simplified graph for identifying soil type. In the work of Campanella et al. (1983), the importance of cone design and the effect of water pressures on the

measurements around unequal end area were evaluated. Therefore, the raw data should be further corrected for pore pressure effect. Significant improvements in classification are made if all three parameters, namely, pore pressure, bearing, and friction ratio, are used (Campanella et al., 1983). Searle (1979) proposed a comprehensive classification chart, similar to the chart proposed by Schmertmann (1978a) but with more details, for use with a mechanical cone. Figure 2-9 can be referenced accurately for low depth soundings as the friction ratio for some fine-grained soils may decrease with increasing effective overburden stress (Robertson and Campanella, 1983).

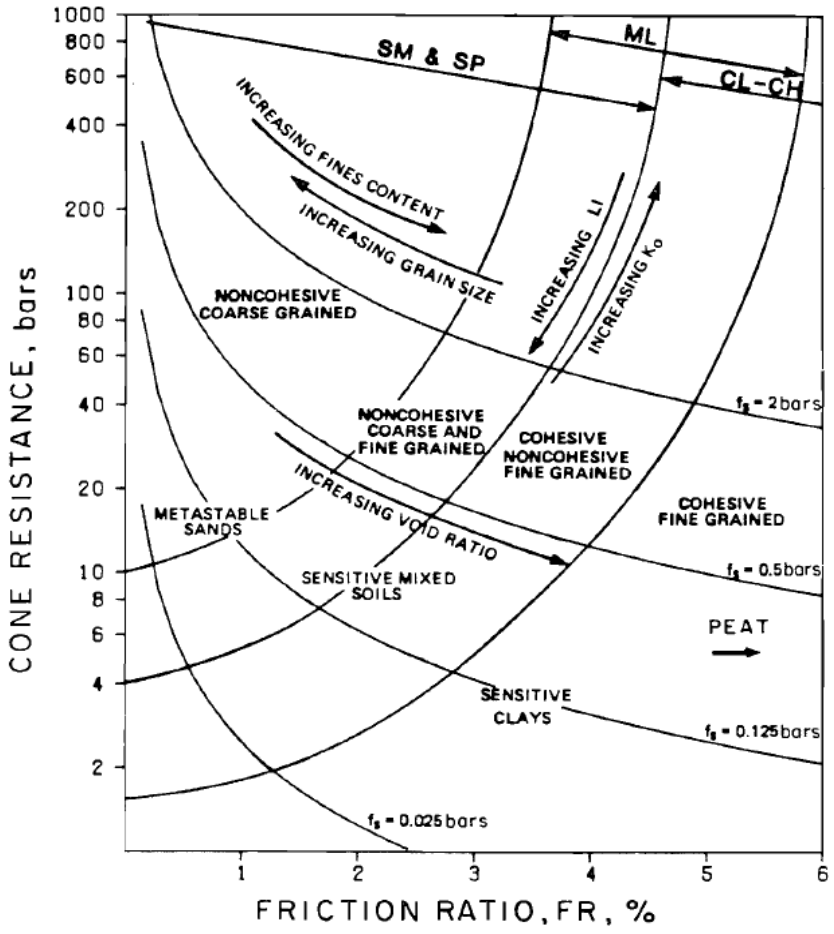

Figure 2-9. Soil classification chart using standard electric friction cone (Douglas and Olsen 1981); 1 bar = 100 kPa

Robertson (2009) developed a simplified CPT-based classification chart shown in Figure 2-10 below for soil behavior type using normalized CPT tip resistance (*Q*) and sleeve friction ratio (*F*).

$$Q = \left(\frac{q_c - \sigma_{vc}}{P_a}\right)\left(\frac{P_a}{\sigma'_{vc}}\right)^n \quad (2\text{-}4)$$

$$F = \frac{f_s}{q_c - \sigma_{vc}} \cdot 100\% \quad (2\text{-}5)$$

The exponent *n* varies from 0.5 in sands to 1.0 in clays. The soil behavior type index *Ic* represents the radial distance between any point on this chart and the point defined by *Q* = 2951 and *F* = 0.06026% (Boulanger, 2014). It often correlates to the fine content (*FC*) in soil classification. Circular arcs defined by constant *Ic* values are used to approximate the boundaries between different soil behavior types in this chart; e.g., *Ic* = 2.05 represents the approximate boundary between soil behavior types 5 and 6, whereas *Ic* = 2.60 represents the approximate boundary between soil behavior types 4 and 5 (Robertson, 2009).

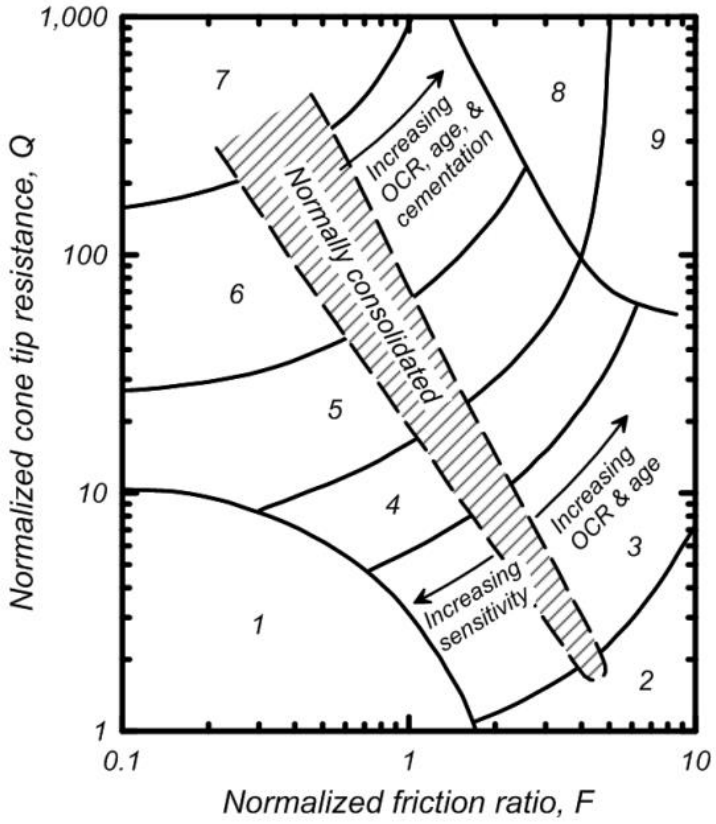

Figure 2-10. Normalized soil classification (Robertson, 2009)

CHAPTER 3 LIQUEFACTION POTENTIAL EVALUATION BY CONE PENETRATION TEST

3.1. Methodology of Liquefaction Potential Characterized by CPT

In this research, cone penetrometer with pore pressure sensor (CPTu) is used to measure the tip resistance, sleeve resistance and pore pressure in the coal slurry. The cone penetrometer is composed of the cone and the extension rod. All the sensors are connected to the computer by the wire from the cone. The hollow rod which has a diameter of 31 mm connects the cone and the wire is inside the rod. It is installed on the C channel of the shake table frame which is located on top of laminar shear box to ensure the verticality. The laminar shear box (LSB) is 2290 by 2130 in mm. The height of the coal slurry in the LSB is around 1300 mm and it limits the depth of the penetration. The penetrating speed is around 2 cm/s and 24 data points are collected from CPTu tests. Therefore, the data analysis of liquefaction and correlation is not affected by the height of the box. The soil in the laminar box is coal slurry and it is kept saturated. Figure 3-1 is the software which records tip resistance, sleeve resistance, and pore water pressure. Figure 3-2 is the setup of CPT on the ground and same setup is used on top of the laminar shear box.

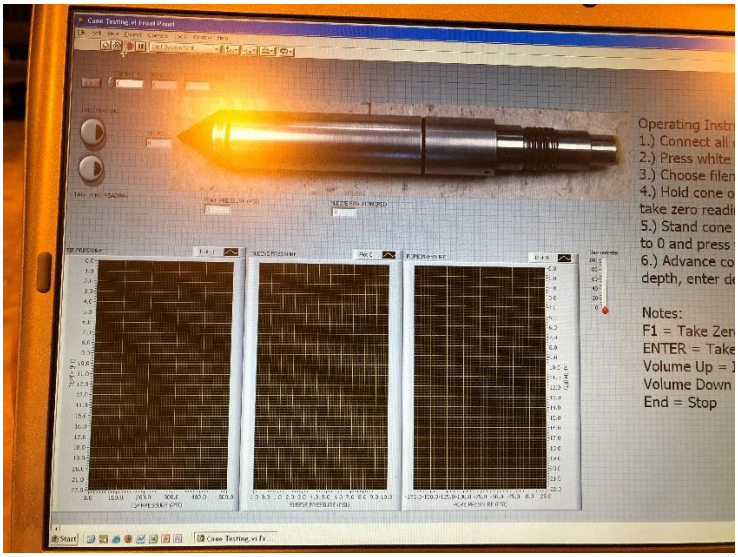

Figure 3-1 Data recording software where tip resistance, sleeve friction and pore pressure are recorded.

Figure 3-2 CPT setup with a diameter of 31 mm cone

3.1.1 Deposition Method of Soil Specimen

The coal slurry was collected and transported from a coal tailing impoundment in eastern Pennsylvania. The coal tailings are mixed with water by a handhold blender in the tank and pumped into the laminar box on the shake table.

The main objective of this thesis is to determine and compare the soil properties of coal slurry retrieved from impoundment. By combining CPT with shake table test, the in-situ soil properties in the impoundment conditions can be simulated. The tip resistance and pore pressure from the CPT is combined with the data measured by the installed accelerometers and piezometers for liquefaction analysis. Furthermore, many soil properties could be derived from CPT tip and sleeve resistance data by using empirical equations, such as pre-consolidation stress, soil classification, and shear modulus. The results obtained from the calculation of normalized CPT data could be further compared with lab testing results to evaluate the accuracy of such unfamiliar material.

The soil properties are obtained by applying a cone penetration test before and after the shaking to get the most accurate in-situ soil properties. By analyzing the data retrieved from CPT, shear modulus, pre-consolidation stress, and soil classification can be derived and the state of soil during and after the seismic event is evaluated. From the calculation, we could evaluate if the soil liquefies during the test.

3.1.2 Analysis of Liquefaction Potential by Cyclic Resistance Ratio and Cyclic Stress Ratio

Cyclic resistance ratio (*CRR*) is generally used to quantify the probability of liquefaction to a specific soil. The earthquake load is defined as the average induced cyclic shear stress ratio (*CSR*). The factor of safety against liquefaction is defined as

$$FS_{liq} = \frac{CRR}{CSR} \tag{3-1}$$

The *CRR* in the equation 3-1 can be determined by the following equation:

$$CRR_{7.5} = 0.833 \times \frac{(q_{c1N})_{cs}}{1000} + 0.05 \; if (q_{c1N})cs \; < 50 \tag{3-2}$$

$$CRR_{7.5} = 93 \times (\frac{(q_{c1N})cs}{1000})^3 + 0.08 \; if \; 50 \leq (q_{c1N})cs < 160 \tag{3-3}$$

where $(q_{c1N})_{cs} = (K_c)(q_{c1N})$, K_c is not be able to evaluated if $I_c \geq 2.6$ $q_{c1N} = Q$ when $Ic >$ 2.6,

$$I_c = [(3.47 - logQ)^2 + (logF + 1.22)^2]^{0.5} \tag{3-4}$$

$$Q = \frac{q_c - \sigma_{vo}}{\sigma_{vo}'} \tag{3-5}$$

$$F = \frac{f_s}{(q_c - \sigma_{vo})} \times 100\% \tag{3-6}$$

Where q_c *is the tip resistance,* σ_{vo} and σ_{vo}' is the total and effective vertical stress in the coal slurry. f_s is the sleeve resistance. I_c is the soil behavior type index. The *CRR* is estimated by results of CPT assuming that the soil experienced 15 cycles of shear.

The $CRR_{7.5}$ could be estimated based on equation 3-2. However, the I_c calculated from CPT results before and after shaking is larger than 2.6 overall and indicated that coal slurry is likely a non-liquefiable soil. Table 3-1 below shows the results of the I_c for all six CPT before shaking and two CPT after shaking. The I_c of CPT2 to CPT4 cannot be calculated due to the negative sleeve resistance from CPT results. The overall I_c of coal slurry is larger than 2.6 with a fine content bigger than 35% from laboratory testing. The coal slurry is considered to be non-liquefiable. However, Chinese criterion defined by Seed and Idriss (1982) will be further used to check if the coal slurry satisfies the conditions of liquefaction.

The simplified equation of calculating *CSR* (cyclic stress ratio) is represented by the normalized CPT tip resistance in equation 3-5 below.

$$CSR = 0.65 \times \frac{a_{max}}{g} \times \frac{\sigma_v}{\sigma_v'} \times r_d \tag{3-5}$$

where the a_{max} is the maximum ground acceleration that set up in the system of shake table. g is the gravitational acceleration. σ_v and $\sigma_{v'}$ is the total vertical stress and effective vertical stress. R_d is the nonlinear shear mass participation factor and it is close to 1 in this experiment. In order to liquefy the coal slurry in the shake table. The a_{max} in equation 3-5 is back calculated where FS_{liq} is smaller than one. Theoretically, CSR should be the same across all the depths of same kind of soil. However, due to the non-uniform deposition, a bigger a_{max} is chosen to make sure all the soil in the shake table liquefies.

3.2 Results and Discussion

3.2.1 Tip Resistance and Sleeve Resistance

Figure 3-4 and Figure 3-5 include all available CPT data. For sleeve resistance, since CPT-2 and CPT-4 have negative values, they are not included in the figure. The negative values may be caused by the suction force of coal slurry. Therefore, they are may not be accurate.

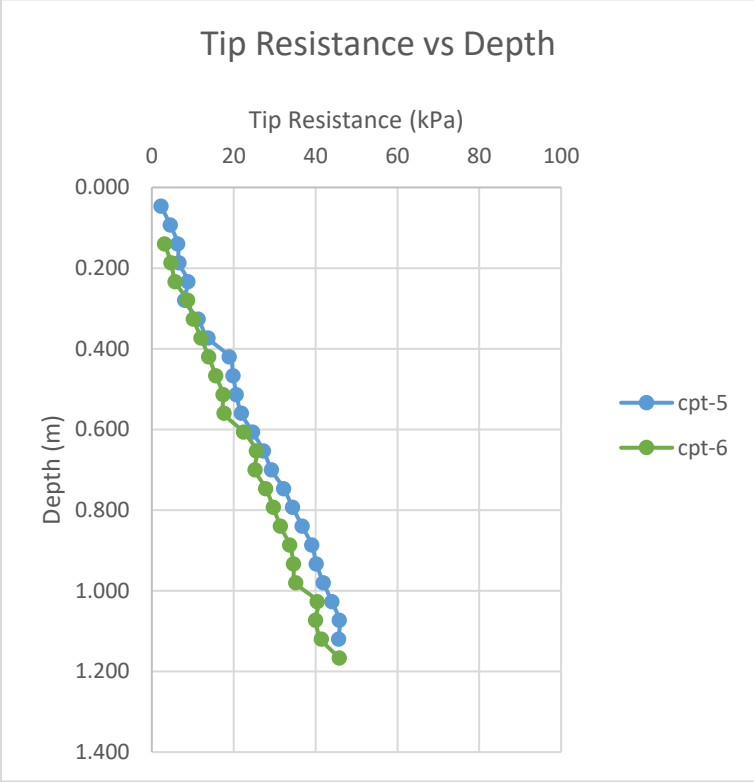

Figure 3-3 Tip resistance from cone penetration

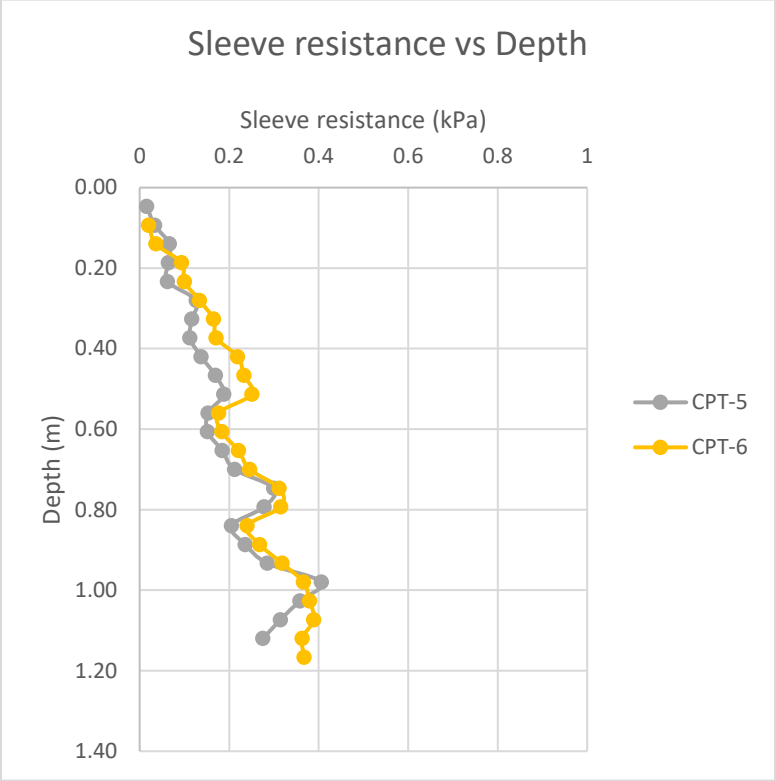

Figure 3-4 Sleeve resistance from cone penetration

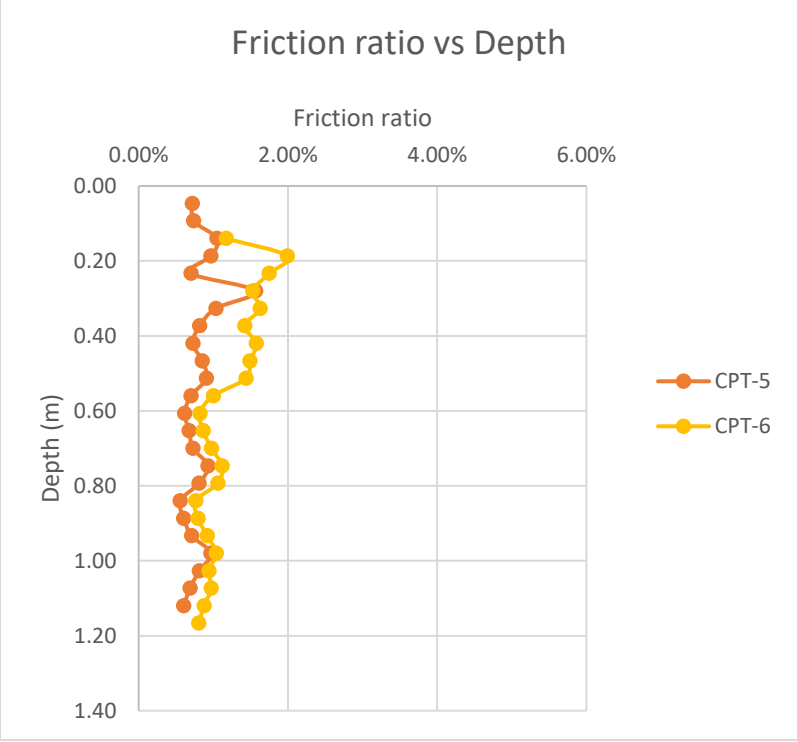

Figure 3-5 Friction ratio vs depth of CPT

Two CPT are preformed after shaking and the results of CPT-6 are compared with the one before shaking in Figures 3-6 to 3-9 below. In the Figure 3-6, tip resistance decreases by 20 kPa at depth of 1.1m in coal slurry. This could be caused by the increase of uniformity of coal slurry after shaking. The particles of coal slurry are distributed more uniformly after 20 cycles of shaking and therefore the tip resistance has decreased. The sleeve resistance hasn't changed after shaking and friction ratio changed due to the change of tip resistance. The most interesting part of comparison is the pore pressure before and after shaking. The CPT-6 after shaking is performed within 10 mins since the shake table stopped moving from 0.15 PGA. The pore pressure after shaking at CPT-6 is much higher than before about 3 kPa. This could be caused by the built up of pore pressure during shaking and it doesn't have enough time to dissipate after the shaking is done. However, piezometers buried in the coal slurry measured a much smaller increase of pore pressure during the shaking, which is around 1kPa at max. The locations of piezometers in coal slurry are different from locations where CPT-6 is performed.

3.2.2 Liquefaction of Coal Slurry

The liquefaction of coal slurry is not observed during shaking by observing the increase of pore pressure measured by piezometers. This phenomenon agrees with the prediction from above I_c calculations where it is larger than 2.6 with a fine content more than 35% in the soil. Also, Chinese criteria defined by Seed and Idriss (1982) can be used to qualitatively evaluate the liquefaction potential of soils with high fine content shown in Figure 3-10. The three conditions for liquefaction occurred in cohesive soils are: 1 The clay content is

smaller than 15% by weight. 2 The liquid limit is smaller than 35%. 3 The natural moisture content is greater than 0.9 times the liquid limit. The grain size distribution from eight samples collected show the clay content is from 10% to 25%. The liquid limit is from 32 to 39 excluding an extreme number. The natural moisture measured from a sample collected in-situ is around 35%, which is greater than 0.9 times the liquid limit. From lab testing results, it is unclear to say the coal slurry is non-liquefied for 100%. However, it doesn't meet all Chinese criterions for a cohesive soil to liquefy.

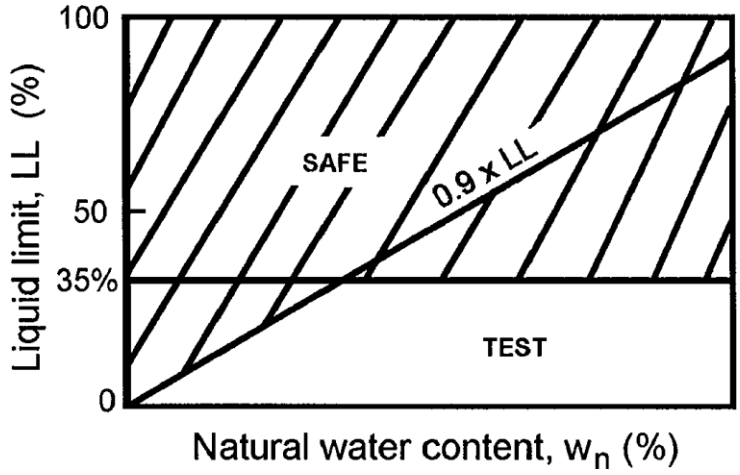

Figure 3-6 Graphical representation of liquefaction criteria for silts and clays from studies by Seed et al. (1973) and Wang (1979) in China (after Marcuson et al. 1990): <15% finer than 0.005mm, liquid limit (LL) < 35%, and water content > 0.9 * liquid limit

3.3 Liquefaction Potential Conclusions

The coal slurry in the laminar shear box does not liquefy during the shaking with a 0.15 PGA. The pore pressure measured from piezometers doesn't climb up to vertical

effective stress of coal slurry during 20 cycles shaking. However, a significant amount of increased pore pressure is observed by cone penetration testing. . The two CPT are performed within 10 mins after the shaking is finished. Smaller tip resistance with same sleeve resistance is measured after shaking at CPT-6. The particles in coal slurry is distributed more uniformly. One more shaking will be performed with a bigger PGA around 0.25g next time to further justify if coal slurry is likely to liquefy due to a larger acceleration.

CHAPTER 4 CORRELATIONS BETWEEN CPT RESULTS AND COAL SLURRY PROPERTIES

4.1 Resonant Column Testing

The resonant column testing is used for obtaining shear velocity and damping ratio of soils. Then, the shear modulus can be derived from shear velocity. The apparatus in the laboratory is a fixed-free end device. It measures natural circular frequency and maximum strain deformation of soil at resonance. Based on the measured frequency and mass polar moment of inertia of soil and driving component, the shear velocity and shear modulus are calculated for dried coal slurry. Eq 4-1 shown below is cited from Das and Luo (2015).

$$\frac{J_s}{J_m} = \frac{\omega_n L}{v_s} \tan\left(\frac{\omega_n L}{v_s}\right) \tag{4-1}$$

where J_s is the mass polar moment of inertia of soil specimen equals to $\frac{1}{2}Mr^2$, M is the mass of soil specimen and r is the radius of soil specimen. J_m is mass polar moment of inertia of top component. ω_n is the angular frequency. L is the length of soil specimen. V_s is the shear velocity calculated from the equation 4-1 above.

4.1.1 Soil Sample Preparation

The soil specimen is prepared using oven-dried coal slurry sieved by 12.5mm opening screen (1/6 of soil specimen diameter) according to ASTM D-4015. Dry pluviation is adopted in reconstitution of specimen to make a homogeneous sample with small range

of void ratio. The method of dropping hammer is used in preparation to make different samples with different void ratios. The first sample is compacted twice with 10 hammer drops. The second sample is compacted four times with 10 hammer drops. The third one is compacted eight times with 10 hammer drops. There are six samples prepared for the test. Three of the specimens are reconstituted using sandy coal slurry collected in the deposition process. The other three specimens are reconstituted using silty coal slurry collected in the deposition process. The gradation curves of two samples are shown in Figure 4-1 and Figure 4-2 below. Total 500g of dried coal refuse is prepared from each coal slurry collection. The coal refuse with sandy appearance has soil particles equals to 67.1% of total weight above #200 and 32.6% below #200. For coal refuse with silty appearance, the soil particles above #200 has 55.9% of total weight and 42.8% of total weight below #200.

In order to minimize the gap between the membrane and the confining walls, the soil specimen is prepared while vacuum is constantly applied. And the setup of vacuum is not changed throughout the entire testing procedures as it affects the resonant frequency of coal specimen. Figure 4-3 shows the configuration of soil sample and driving component. There are four magnets and an accelerometer on the top connected to the computer with a black wire. The applied air confining pressure to all six tests is from 75 kPa to 85 kPa with an average of 80 kPa. The set confining pressure corresponds to a depth of 5.71m in saturated coal slurry with a unit weight of 14 kN/m^3.

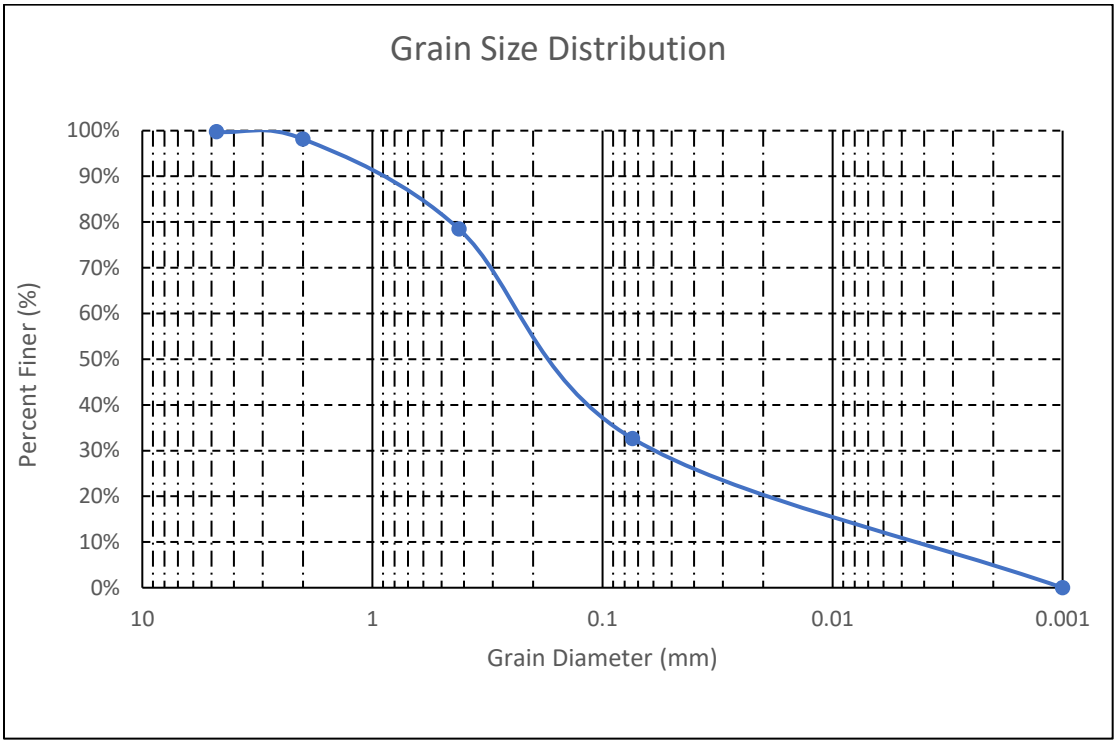

Figure 4-1 Gradation of coal slurry with higher sand content

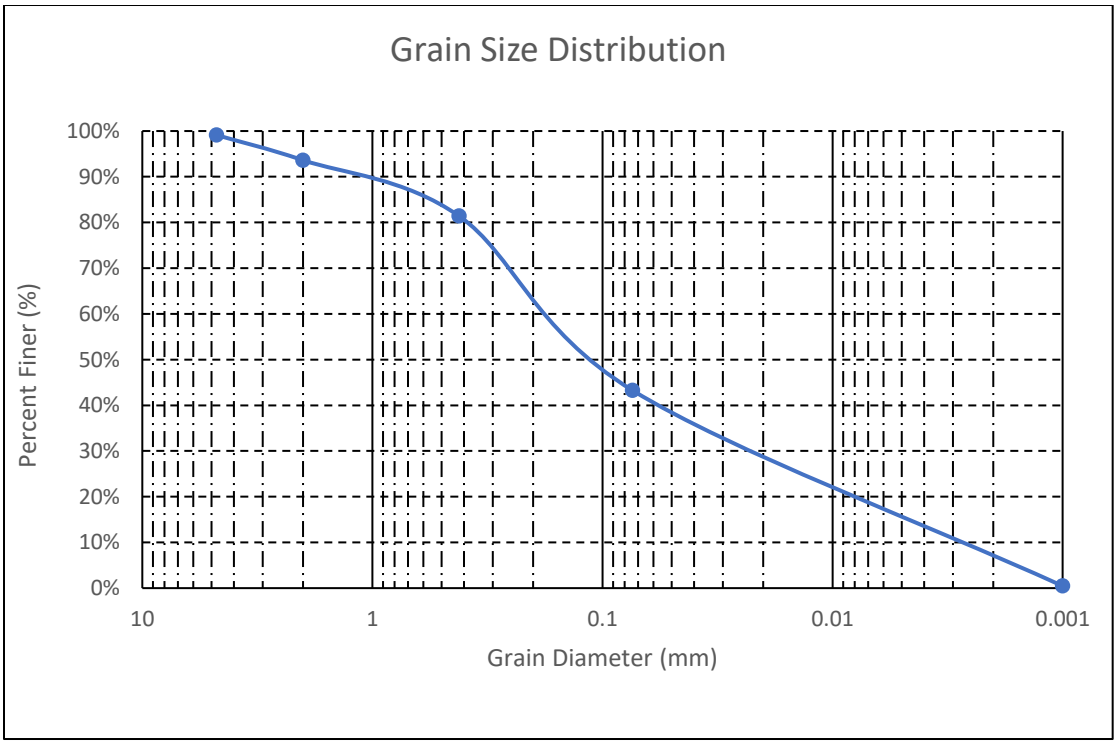

Figure 4-2 Gradation of coal slurry with higher fine content

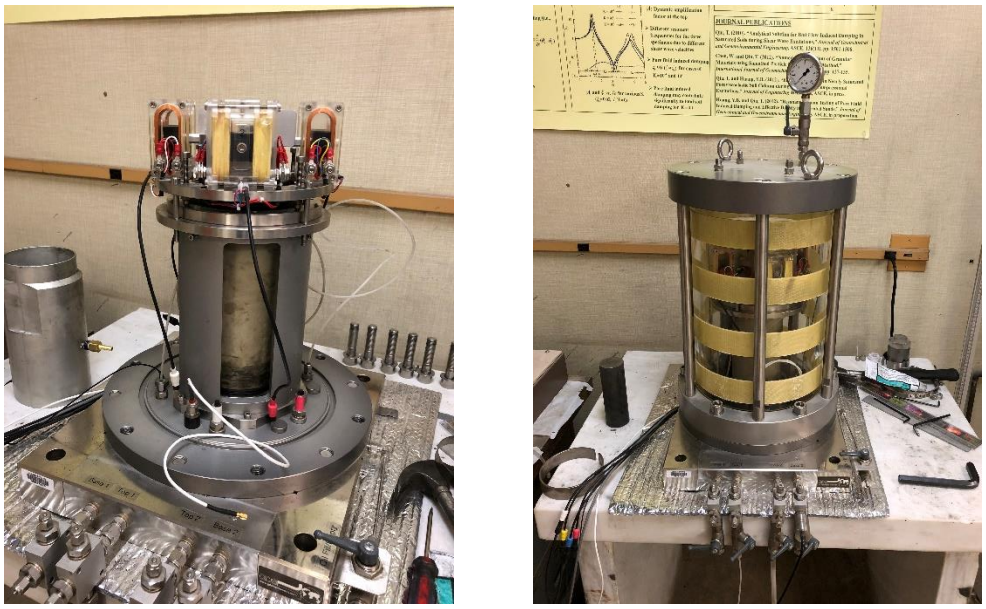

(a) Sample assembling (b) Pressure chamber installed

Figure 4-3 Resonant column sample preparation and testing.

4.1.2 Soil Parameters and Resonant Column Testing Results

Figures 4-4 to figure 4-9 shows the resonance frequency of different soil samples with different void ratios.

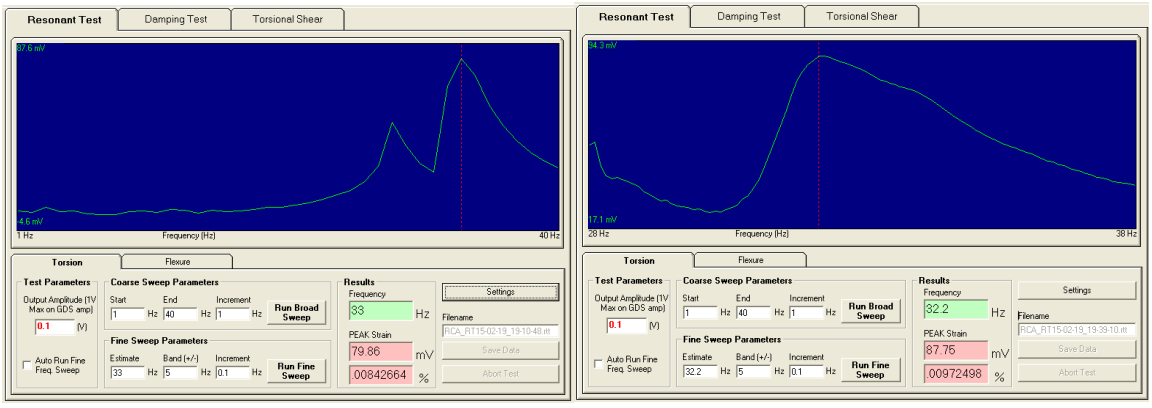

Figure 4-4. Frequency at resonance with peak strain, sandy coal slurry with void ratio equals to 1.074.

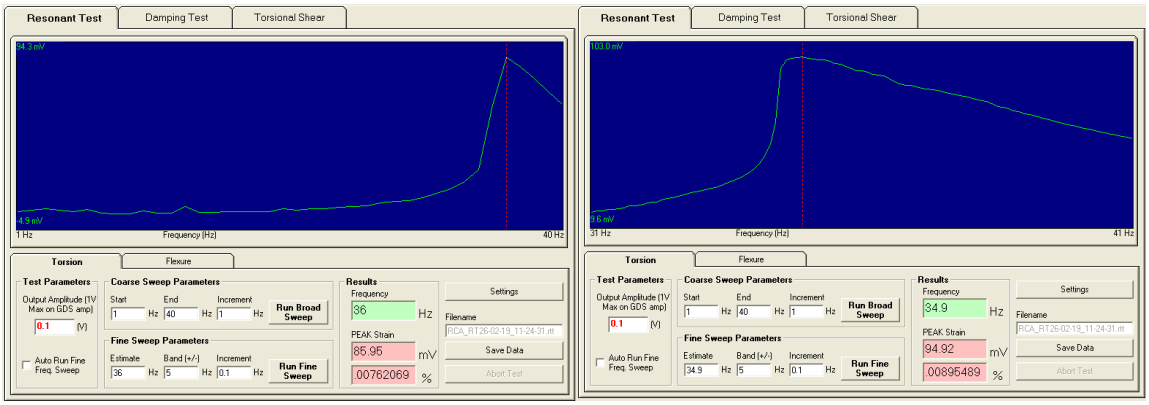

Figure 4-5. Frequency at resonance with peak strain, sandy coal slurry with void ratio equals to 0.755.

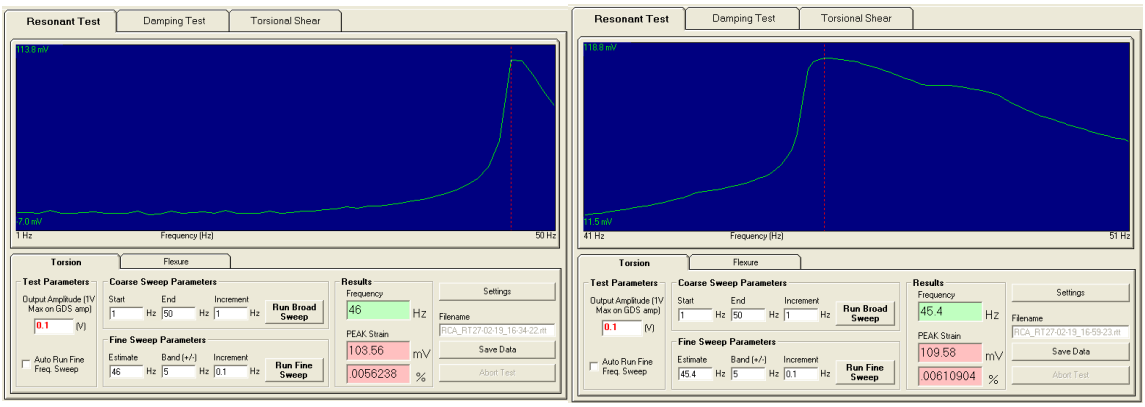

Figure 4-6. Frequency at resonance with peak strain, sandy coal slurry with void ratio equals to 0.689.

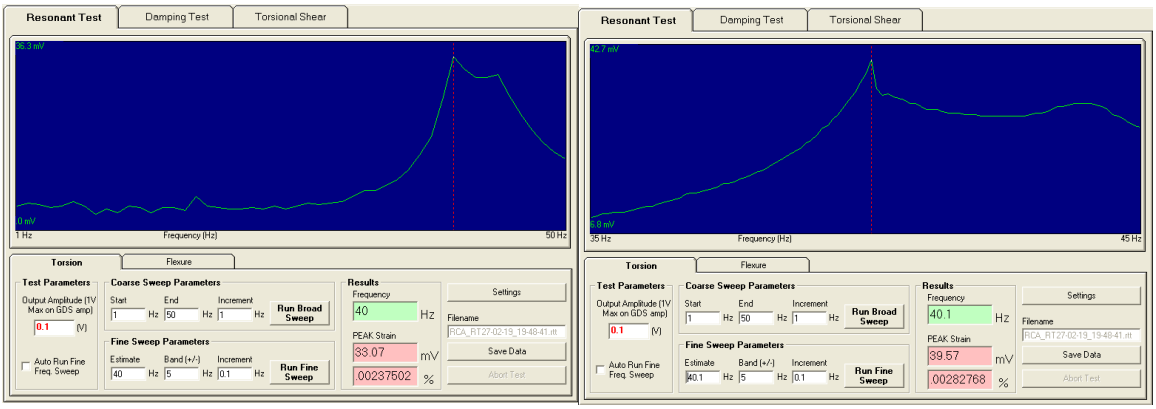

Figure 4-7. Frequency at resonance with peak strain, sandy coal slurry with void ratio equals to 0.956.

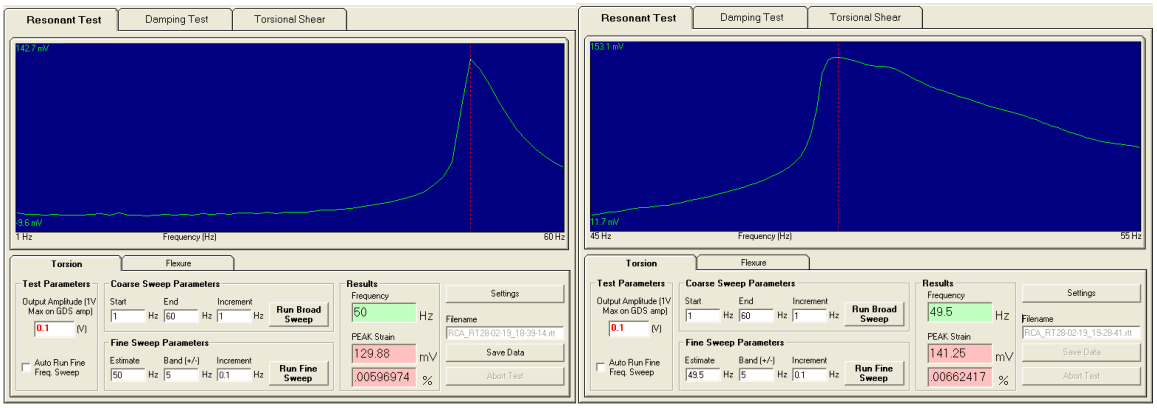

Figure 4-8. Frequency at resonance with peak strain, sandy coal slurry with void ratio equals to 0.878.

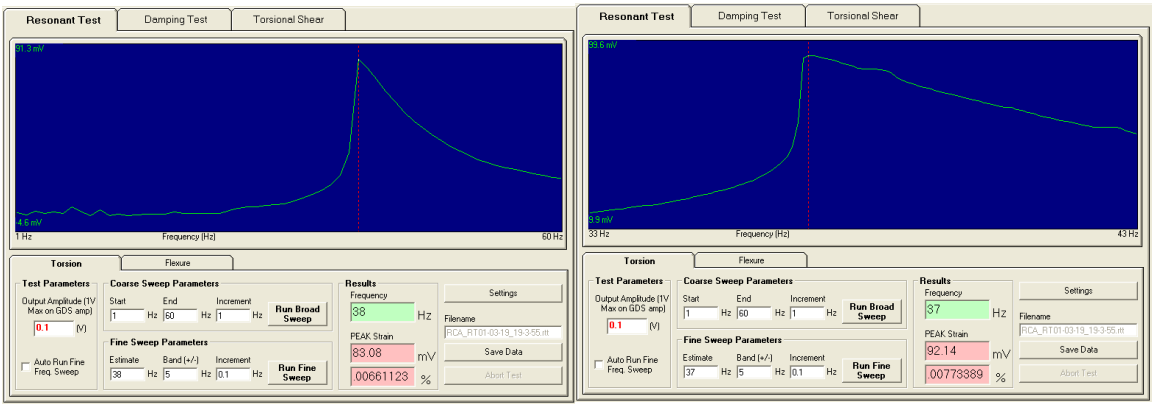

Figure 4-9. Frequency at resonance with peak strain, sandy coal slurry with void ratio equals to 0.774.

The dimensions of specimens and dynamic properties of the coal slurry in resonant column testing are illustrated below in Table 4-1. The void ratio of the soil specimens has been targeted to vary from 0.6 to 1.2 during sample preparation to develop exponential trend lines. The top component consists of four magnets and four metal arms. Its mass polar moment of inertia is calibrated by Sasanakul (2005) with lab testing and numerical analysis. The resonant column apparatus in her research has same top component and dimensions as ours. Therefore, polar moment of inertia of driven plate calibrated from 14 Hz steel rod is cited in this research for calculation of shear velocity and shear modulus. In the results, the shear velocity increases along with decreasing void ratio. The trend of the data is presented in Figure 4-10. The dried coal refuse with higher fine content has bigger shear wave velocity compared to the dried coal refuse with less fine content. The shear modulus of coal refuse is estimated based on the dried density of soil sample prepared in the column and the shear velocity calculated from resonant frequency. The results of two coal refuse are drawn in the Figure 4-11. In the figure, coal refuse with less fine content has smaller shear modulus along with smaller void ratio. Coal refuse with higher fine content has larger shear modulus with decreasing void ratio.

Table 4-1 Resonant column raw data and results

Coal Slurry	Sandy Coal Refuse			Silty Coal Refuse		
mass (kg)	1.454	1.763	1.832	1.582	1.6476	1.744
length (m)	0.192	0.197	0.197	0.197	0.197	0.197
radius (m)	0.05	0.05	0.05	0.05	0.05	0.05
void ratio	1.074	0.755	0.689	0.956	0.878	0.774
frequency (Hz)	32.2	34.9	45.4	40.1	49.5	55
dried density (kg/m^3)	964.2	1139.5	1184.0	1022.5	1064.9	1127.2
J_{dp} ($kg\text{-}m^2$)	8.934E-05	8.934E-05	8.934E-05	8.934E-05	8.934E-05	8.934E-05
J_{cap} ($kg\text{-}m^2$)	1.519E-03	1.519E-03	1.519E-03	1.519E-03	1.519E-03	1.519E-03
J_{soil} ($kg\text{-}m^2$)	1.818E-03	2.204E-03	2.290E-03	1.978E-03	2.060E-03	2.180E-03
β	0.8989	0.9598	0.9720	0.9256	0.9385	0.9564
Vs (m/s)	43.21	45.01	57.81	53.62	65.29	71.18
G (MPa)	1.801	2.308	3.958	2.940	4.539	5.711

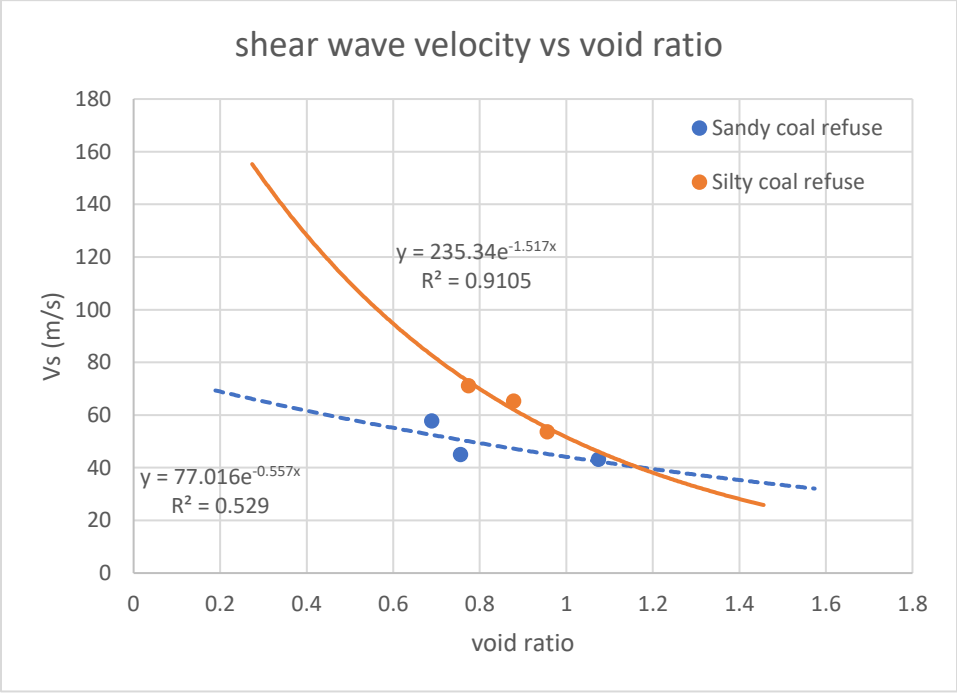

Figure. 4-10 Dried coal slurry shear velocity vs void ratio

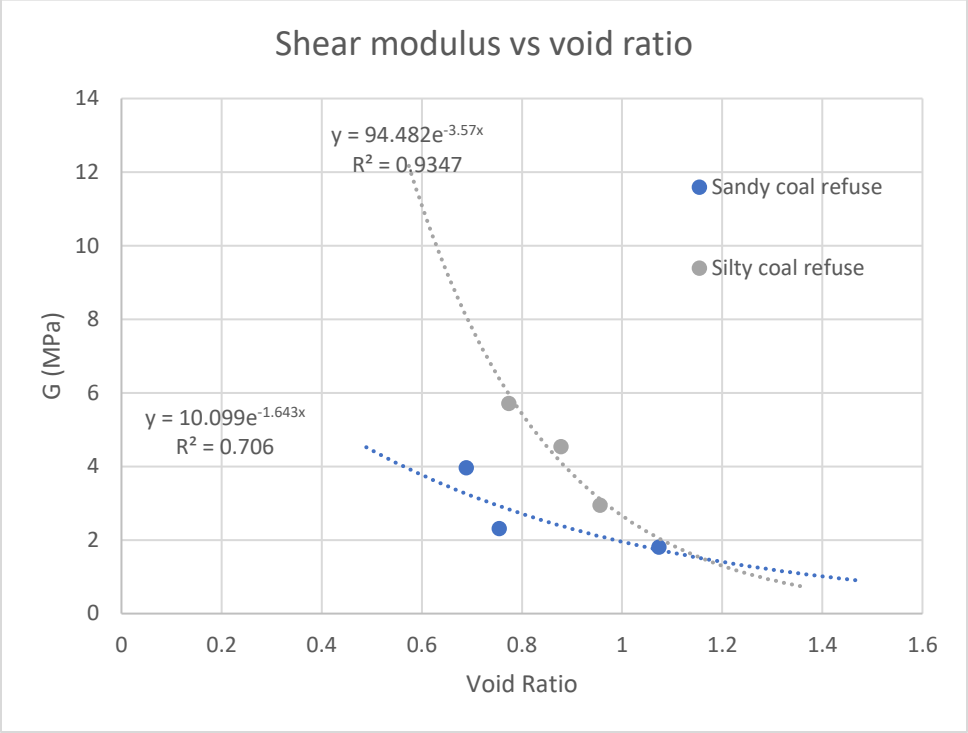

Figure 4-11 Dried coal slurry shear modulus vs void ratio

4.1.3 Coal Slurry's Dynamic Properties Derived from CPT

Hegazy and Mayne (1995) found that V_s in sands and clays can be correlated with q_c and void ratio e_o and updated the correlations using additional data. More recently, Suzuki et al. (1998) found that normalization of the V_s to the corrected cone tip resistance in Japanese sites had a trend with the soil behavior type index (I_c). A globally statistical correlation to estimate V_s in any soil type using cone data by Hegazy and Mayne (2006) is used in this research. The V_{s1} is the corrected V_s to a reference overburden stress according to Robertson et al. (1992)

$$V_{s1} = V_s \times \left(\frac{P_a}{\sigma'_{vo}}\right)^{0.25} \quad (4.2)$$

where

$$V_{s1} = q_{c1N} * 0.0831 * e\text{^}(1.786 * I_c) \quad (4.3)$$

Then the shear modulus of coal slurry is estimated from correlated shear wave velocity by Equation 4-4 shown below:

$$G = \rho_{sat} \times v_s^2 \quad (4\text{-}4)$$

The saturated density of coal slurry in laminar box is estimated based on the unit weight of slurry around 1428.6kg/m^3. The I_c is calculated in the same way presented in chapter 3 and all units are in kPa and m/s.

The correlated shear modulus from CPT results is shown in Figure 4-12. CPT5-CPT6 before and after shaking have trends from 0 to 3 MPa from the surface of coal slurry to the bottom of laminar box. The correlated shear modulus for CPT2 to CPT4 can't be calculated due to a negative sleeve resistance. CPT1 has several peaks of correlated shear modulus. This could be caused by the deposition process since the whole deposition is completed from five stages and each stage has a four days gap.

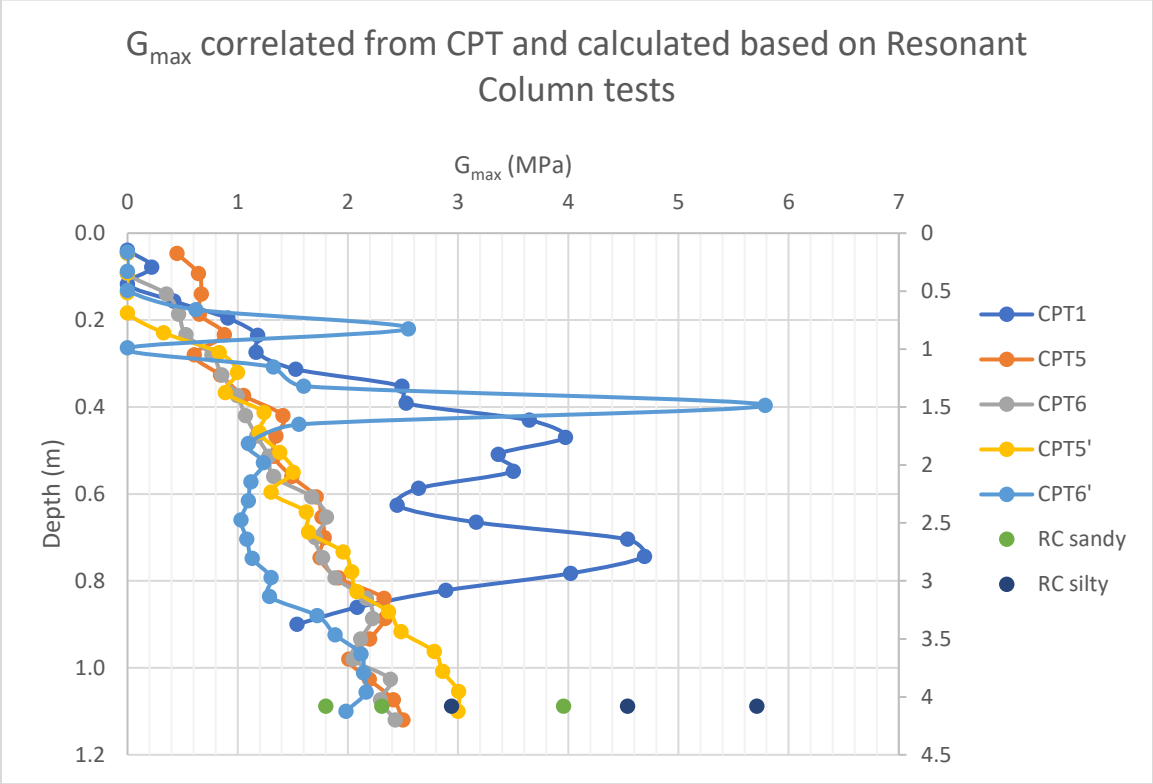

Figure 4-12 *Gmax* derived from CPT and resonant column (RC) tests.

4.1.4 Compare and Contrast of Coal Slurry Dynamic Properties Derived from Resonant Column Testing and CPT

The shear modulus derived from resonant column testing is 1.8 to 3.9 MPa for dried sandy coal refuse and 2.9 to 5.7 MPa for dried silty coal refuse with the void ratio between 0.69 to 1.07. The confining pressure of resonant column test is around 80 kPa, which equals to 4.08m below the ground surface of saturated coal slurry. Due to the non-uniform deposition in the laminar shear box, the void ratio of coal slurry can be different at different locations.

The correlated shear modulus from CPT 1 has a correlated shear modulus along with the ununiform distribution of coal slurry particles. The shear modulus derived from CPT is around 2 MPa at a depth of 0.85m. There are two possible reasons which can be used for the difference in the two methods. First, the coal slurry in the resonant column test is under dried condition. The voids between particles are filled by air. The density of dried coal refuse is smaller than that saturated coal refuse and shear wave velocity is smaller too. Therefore, the shear modulus from resonant column testing should be smaller than the derived shear modulus from CPT results due to dried condition. The correlated shear modulus from CPT5 and CPT6is close to the correlated shear modulus from CPT tests after the shaking. . The coal slurry contains more silty particles than sandy particles at these two locations. As shown in Figure 4-12, the shear modulus from resonant column testing also generally increases with the increase of silt content.

Second, the dried coal slurry in the resonant column tests is sieved by a 12.5mm screen based on the ASTM specification that the particle size in the specimen should be smaller than 1/6 of the specimen's diameter. This process filters many large coal particles out of the specimen. However, the coal slurry in the laminar shear box has particle size up to 1cm Therefore, the larger coal particles may increase the tip resistance of CPT and the correlated shear modulus. Lastly, equation 4-2 is an empirical equation for sandy soil. Although coal slurry has more than 50% sandy particles, its fine content is also high. The silty and clayey particles make coal slurry soft but with higher sleeve resistance. Therefore, the shear modulus could be more accurately estimated if the constant in equation 4-2 is adjusted based on coal slurry's properties.

4.1.5 Conclusions and Suggestion

Future research is necessary for establishing the correlation of shear modulus for coal slurry based on CPT results. The comparison can be more representative if the specimens of resonant column is saturated with a smaller confining pressure and the CPT is performed in-situ with a deeper depth.

4.2 Consolidation Testing

Table 4-2 Coal slurry parameters from consolidation test

Sample Location	Depth, z (m)	Compression Index, c_c	Swell Index, c_s	Coefficient of consolidation, C_v (cm^2/min)
Jeddo 8 Boring 1	1.5	0.242	0.007	0.75
	4.6	0.453	0.010	2.36
	7.6	0.200	0.013	0.89
Jeddo 14 Boring 1	1.5	0.234	0.005	1.06
	4.6	0.134	0.003	1.70
	10.7	0.200	0.013	1.17

Consolidation test is performed to obtain coal slurry's pre-consolidation stress. The pre-consolidation stress is the maximum effective stress that a soil has sustained in the past. It is determined using the Casagrande's graphical method in this experiment. Although void ratio versus linear effective stress is more common than vertical strain versus linear effective stress, the second method that was developed by Sallfors (1975) is adopted here. Both methods yield similar pre-consolidation stress. Upon applying this method in Figure 4-11, the soil specimen from Jeddo 8 boring 1 has pre-consolidation stress of 24 kPa. From

Figure 4-12, the soil specimen from Jeddo 14 boring 1 has pre-consolidation stress of 28 kPa.

The compression index c_c , swell index c_s, and coefficient of consolidation C_v are included in Table 4-2. Soil samples are retrieved from different depths on the site from two different coal slurry impoundments. The coal slurry properties can be estimated based on the soil index.

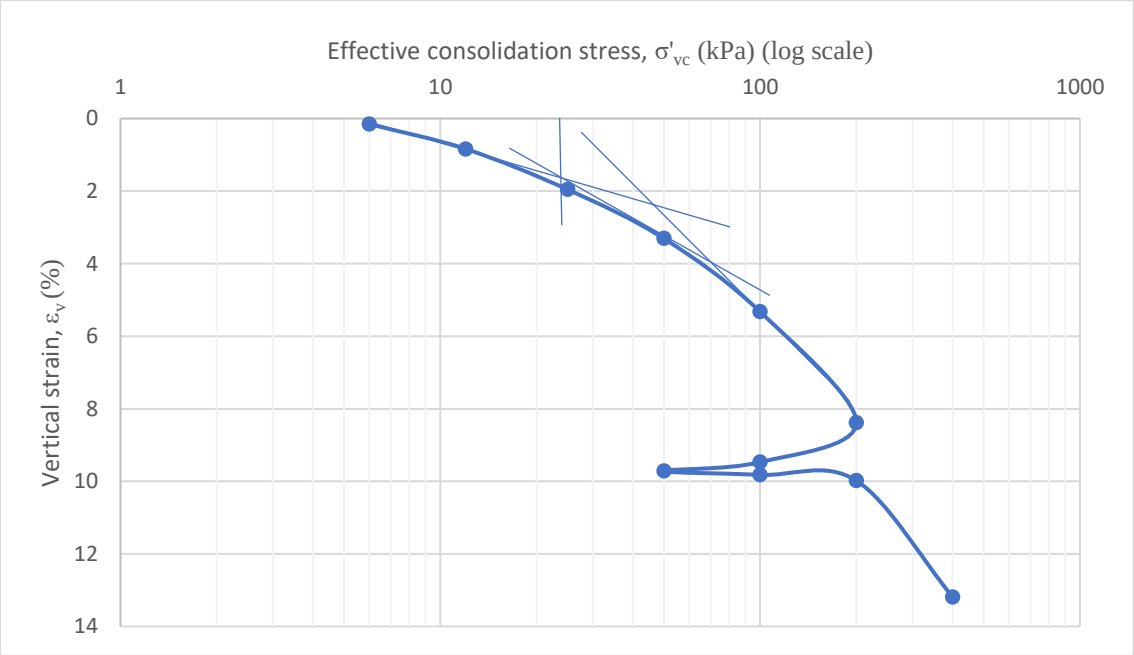

Figure 4-13 Percent consolidation versus linear effective stress, sample collected from depth of 1.5 m.

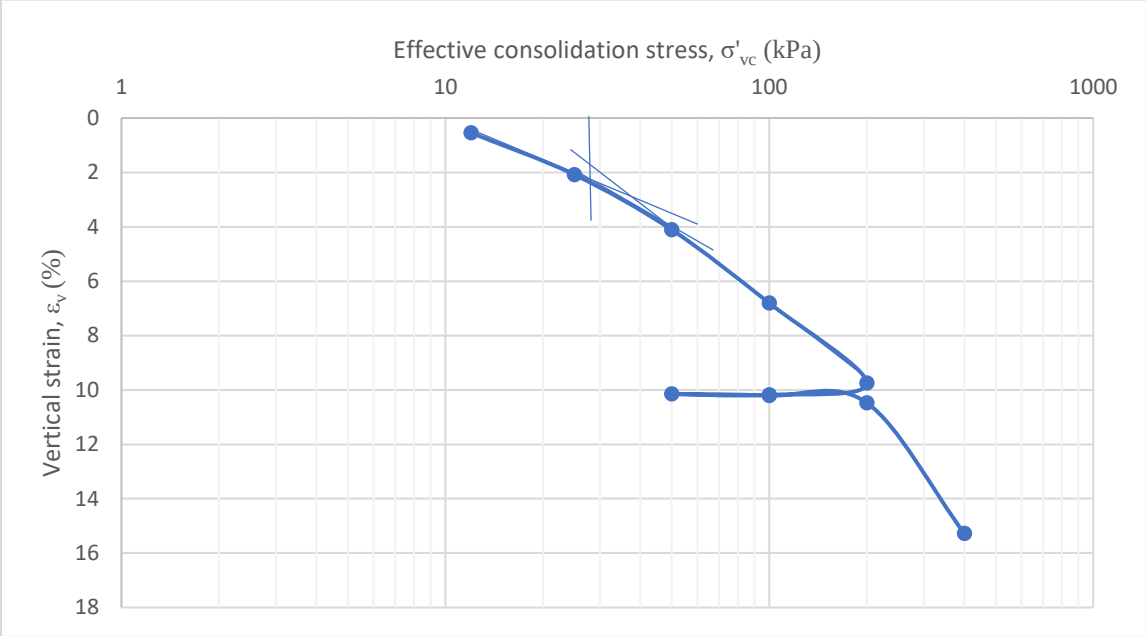

Figure 4-14 Percent consolidation versus linear effective stress, sample collected from depth of 1.5m.

In order to establish the correlation between CPT and soil stress history of consolidation, typical values are cited from Table 4-3. The table lists typical ranges of the effective shear strength parameters, friction (tanϕ') and attraction (a) for common soil types (Senneset, 1985). Two parameters over a stress range $\Delta\sigma$' are defined by the Mohr-Coulomb failure criterion in Figure 4-15. Shear strength τ_f can be approximated by equation 4-4.

$$\tau_f = (\sigma' + a)tan\phi' \tag{4-4}$$

where τ_f denotes shear strength and σ' denotes effective normal stress on the failure plane. The term attraction (a) is the negative intercept of the normal stress axis and the cohesion (c) is relation to the attraction by:

$$c = a \times \tan(\phi') \quad (4\text{-}5)$$

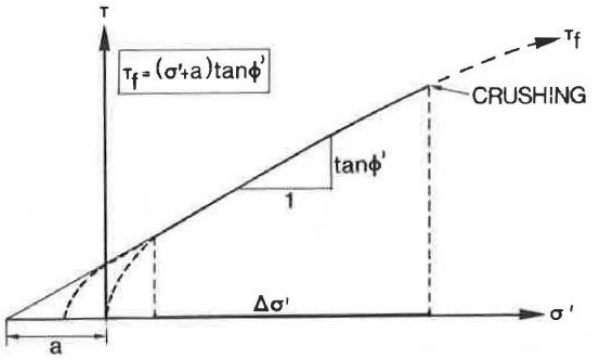

Figure 4-15 Strength parameters in the Mohr-Coulomb criterion (Senneset, 1985).

Table 4-3 Typical values of attraction (a) and friction (tanϕ') (Senneset, 1985).

	Shear Strength Parameters				
	a(kPa)	tan ϕ'	ϕ'	N_m	Bq
Clay					
Soft	5-10	0.35-0.45	19-24	13	0.8-1.0
Medium	10-20	0.40-0.55	19-29	35	0.6-0.8
Stiff	20-50	0.50-0.60	27-31	58	0.3-0.6
Silt					
Soft	0-5	0.50-0.60	27-31		
Medium	5-15	0.55-0.65	29-33	5-30	0-0.4
Stiff	15-30	0.60-0.70	31-35		
Sand					
Loose	0	0.55-0.65	29-33		
Medium	10-20	0.60-0.75	31-37	30-100	<0.1
Dense	20-50	0.70-0.90	35-42		
Hard, stiff soil OC, cemented	>50	0.8-1.0	38-45	100	<0

Coal slurry shear strength parameters a is estimated as 20 kPa and tan ϕ' is 0.6. This number is based on the fine contents of this material and its possible coal particles. Both parameters are used in the calculation of pre-consolidation of coal slurry based on CPT tip resistance. The coefficient N_{qec} is estimated based on the soil type and tan ϕ' in Figure 4-16. Since there is an error of percentage for the coefficient, the pre-consolidation is within a small range. The pre-consolidation is calculated based on equation 4-6.

$$\sigma_c' + a = \frac{q_T' + a}{N_{qc}} \tag{4-6}$$

where σ'_c is the pre-consolidation stress, q'_T is the effective cone resistance defined as $q_T' = q_T - u_T$ and N_{qc} is the bearing capacity coefficient.

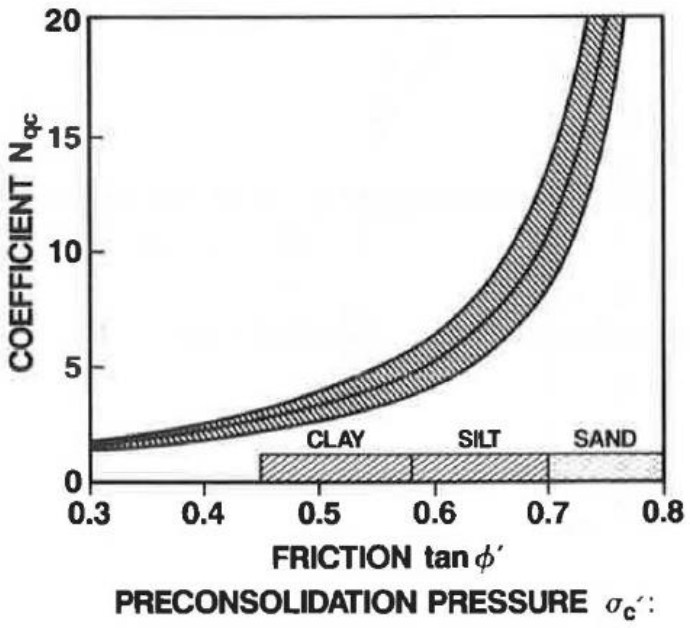

Figure 4-16 N_{qc} and tanϕ' (Senneset, 1985)

In order to correlate the CPTu results to pre-consolidation stress of coal slurry, shear strength parameters are estimated based on soil properties. Attraction *a* is estimated as 20 kPa based on the fine content of coal slurry and N_{qc} is estimated as 8 based on Figure 4-16. The blue points in Figure 4-17 is the approximated pre-consolidation derived from equation 4-6. The orange line is composed by two points from results of oedometer tests. The samples of oedometer test are retrieved from 0-5 feet below the ground surface. Equation 4-6 can be adjusted based on coal slurry since the soil is under-consolidated and the tip resistance from CPT is too small. The void ratio for in-situ coal slurry samples varies from 0.7 to 1.0 where void ratio of coal slurry in laminar box is around 1.4.

Table 4-4 Pre-consolidation stress from lab testing and correlation

Depth (m)	Correlated from CPT (kPa)	Oedometer Test (kPa)
1.52	22.48	24
1.52	24.25	28

From Table 4-4, the pre-consolidation stress of coal slurry from correlated CPT results is smaller than oedometer testing results. The correlated pre-consolidation has a varying value of pre-consolidation across the penetration due to increasing tip resistance. This could be caused by the increase of sandy particles in coal slurry in the middle of the slurry deposit due to the non-uniformity of the coal slurry in the deposition process. The approximation of pre-consolidation stress from oedometer data with graphical determination can affect the values in Table 4-4. The pre-consolidation stress from different CPT tests is varying with changing tip resistance. However, the correlated pre-

consolidation stress from CPT results and pre-consolidation stress from oedometer testing of coal slurry generally agree with each other.

4.3 Soil Classification

The CPT-soil classification chart shown in Figure 4-18 by Douglas and Olsen (1981) shows three zones of different soil-behavior types. Data of the cone resistance and friction ratio from CPT are used to estimate the soil type based on Figure 4-18. There are six sets of CPT data retrieved from different locations of laminar box. These data points in Figure 4-19 gathered below 0.05 MPa at 1.5% friction ratio. Taken the reference from Figure 4-18, the coal slurry can be classified as CL-CH and the sleeve friction is below 0.5 kPa.

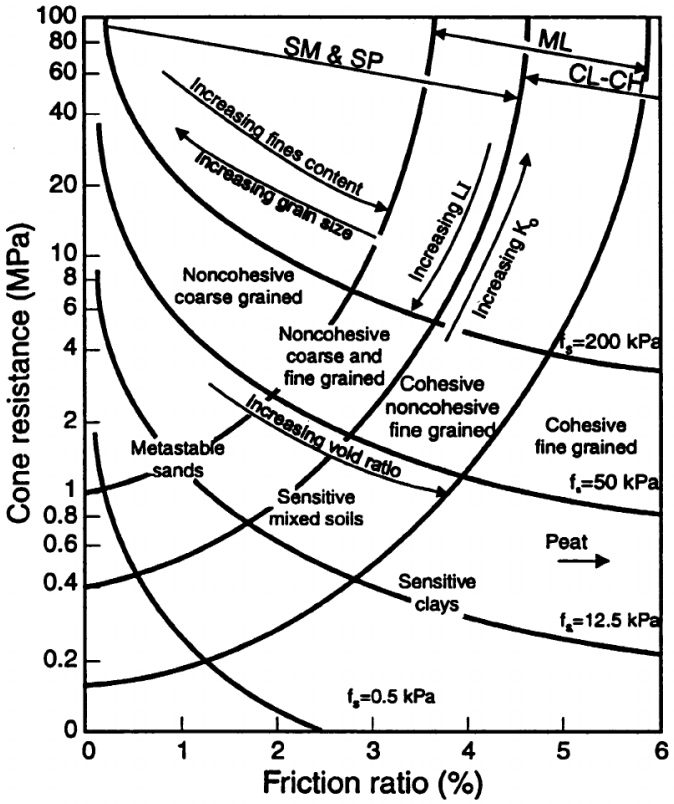

Figure 4-17. CPT Soil Behavior Type Classification Chart (Douglas and Olsen, 1981)

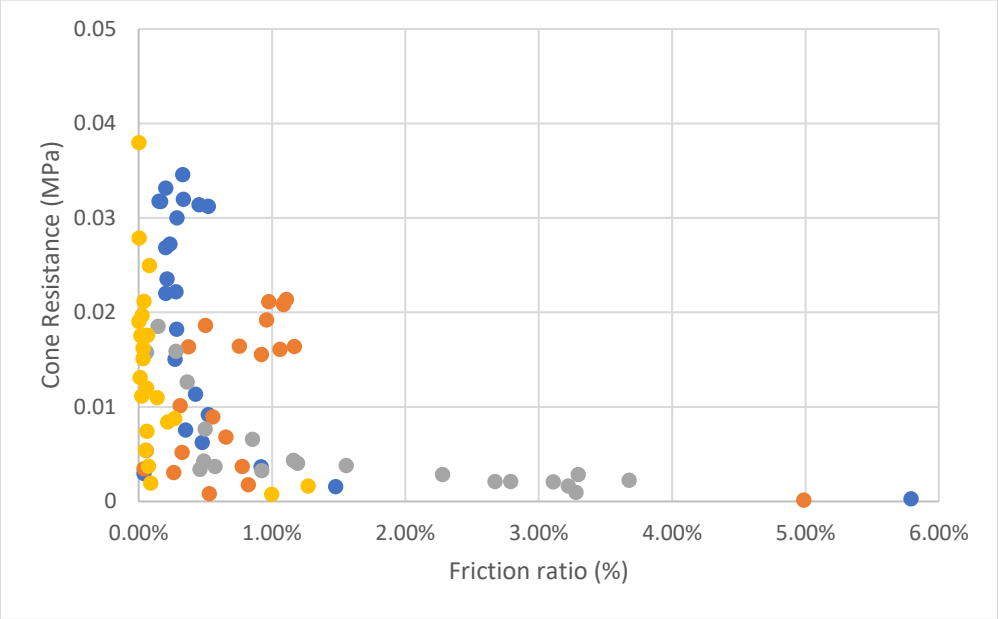

Figure 4-18. Tip Resistance vs. Friction ratio of coal slurry

The lab testing of coal slurry matches the results from correlations of CPT testing. The particle distribution is obtained by performing sieve analysis and hydrometer test. Combining with PL (plastic limit) and LL (liquid limit) from Atterberg limit test, the coal slurry is classified by the USGS classification standard and the results are shown in table 4-4. Grain size distributions of coal slurry from lab testing are attached in Figure 4-20.

Table 4-5. Soil classification from lab testing

	LL	PL	PI	Classification	
D1S1	55.4	35	20.0	CH	Elastic silt
D1S2	39.4	29	10.8	CL	Sandy Lean Clay
D3S1	35	33	1.7	ML	Silt
D3S2	36	29	6.2	CL-ML	Silty Clay
D4S1	33	28	5.5	CL-ML	Silty Clay

D4S2	37	28	9.9	Cl	Lean Clay
D5S1	33	32	1.2	ML	Silt
D5S2	32	28	3.7	ML	Silt

Table 4-6. Comparison of soil classification

Soil Type	Soil classification from lab testing	Soil classification from correlated CPT results
Coal Slurry	CL-ML	CL-CH

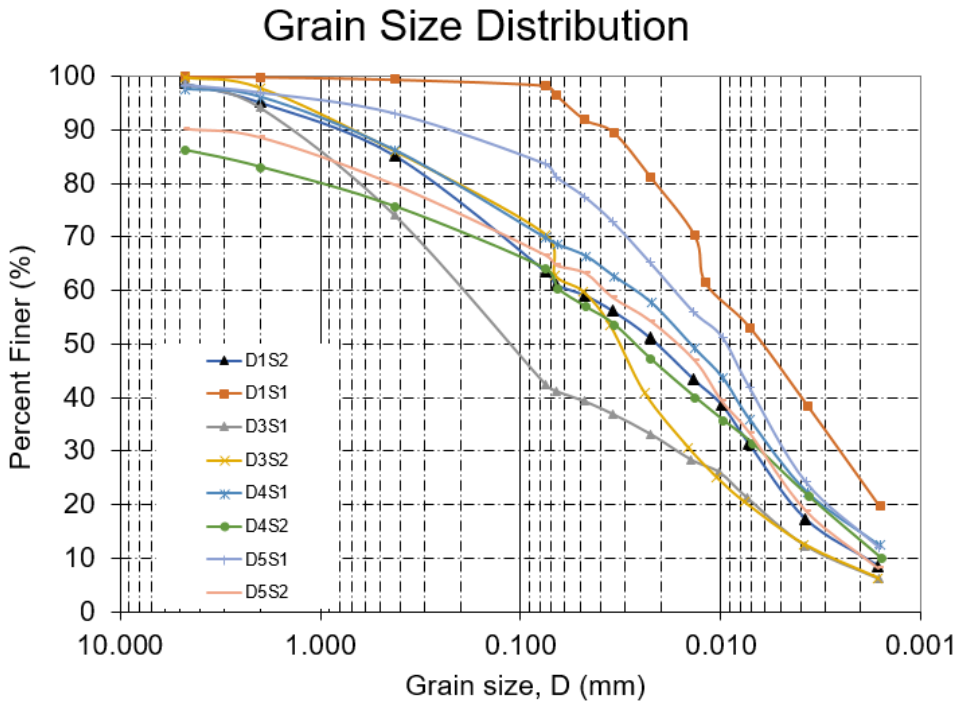

Figure 4-19 Grain size distributions of coal slurry in laminar shear box

The D1S1 represents the sequence of depositions and number of samples where D1 means first deposition of coal slurry and S1 means sample 1 retrieved from first deposition. The coal slurry in laminar box is deposited in five layers due to its large quantity. Due to its high fine content and low plasticity index, the coal slurry is classified as CL and ML

mostly from the lab testing. The tip resistance of silty and clayey particles from CPT is very small and the correlated points are clustered at the lower left in Figure 4-18 where soil is classified as CL-CH. The correlated soil classification agrees with laboratory testing in general.

The coal slurry in the laminar shear box is not entirely homogeneous across all layers. The non-uniform deposition process makes the tip resistance in the center of the laminar box larger than the tip resistance from the corner. Also, the sleeve friction is smaller in the center compared to the sleeve friction in the corner. This can explain the discrepancy of soil classification derived from CPT comparing to the lab testing results.

CHAPTER 5 CONCLUSIONS

This research focuses on evaluating liquefaction potential of fine coal refuse using CPT and correlations of soil properties with CPT test results. This study aims to collect the geotechnical properties of fine coal refuse such as cyclic resistant ratio, shear modulus, pre-consolidation stress, and soil classification. The properties of fine coal refuse obtained in laboratory have been compared to the CPT results. Therefore, the properties of fine coal refuse can be estimated based on in-situ CPT in the future. The key findings from this study are presented as follows.

1. The liquefaction of coal slurry is not observed during shake table testing with a 0.15g PGA. This agrees with the liquefaction factor of safety calculation. Also, the coal slurry doesn't meet all requirements in Chinese criteria for a cohesive soil with high fine content to liquefy. However, an increase of pore pressure is observed in CPTu testing and a larger a_{max} will be applied to shake table to further justify if coal slurry is still not be able to liquefy under cyclic loading.
2. The shear modulus of coal slurry reconstituted in a laminar shear box is correlated by cone penetration test and compared with the results obtained from resonant column test. The difference of shear modulus can be partially explained by the status of coal refuse during the test. The general trend of results agrees with the shear modulus of common soil under saturated and dried conditions.
3. The pre-consolidation stress of coal slurry is estimated based on correlated cone penetration test. It is then compared to the pre-consolidation stress measured from

consolidation test of coal slurry from representative in-situ fine coal slurry. The trend between them is close to each other. The pre-consolidation stress correlated from cone penetration test is calculated based on empirical equation for sand. Therefore, the error can be minimized with an empirical equation specifically for coal slurry.

4. The soil classification of fine coal slurry is also correlated by the cone penetration test and compared with laboratory testing such as sieve analysis, hydrometer test, and Atterberg limits. Both approaches have similar soil classification result.

REFERENCES

Timothy D. Stark, and Scott M. Olson (1995). "Liquefaction Resistance Using CPT and Field Case Histories." *Journal of Geotechnical Engineering*, Vol. 121, No. 12, ASCE.

Robertson, P.L. and (Fear) Wride, C.E. (1998). "Evaluating cyclic liquefaction potential using the cone penetration test." *Canadian Geotechnical Journal*, Vol. 35, No.3, 442-459.

Robertson, P.K., Woeller, D.J. and Finn, W.D. (1992). "Seismic cone penetration test for evaluating liquefaction potential under cyclic loading." *Canadian Geotechnical Journal*, Vol.29, No.4, 686-695.

Youd, T.L. and Idriss, I.M. (2001). "Liquefaction resistance of soils: Summary report from the 1996 NCEER/NSF workshops on evaluation of liquefaction resistance of soils." *Journal of Geotechnical and Geoenvironmental Engineering*, ASCE, Vol. 127, No. 4, 297-313.

P.K. Robertson, (2015). "Comparing CPT and V_s Liquefaction Triggering Methods." *Journal of Geotechnical and Geoenvironmental Engineering*, ASCE.

Andrus, R. D., Mohanan, N. P., Piratheepan, P., Ellis, B. S., and Holzer, T. L. (2007). "Predicting shear-wave velocity from cone penetration resistance." *Proc., Earthquake Geotechnical Engineering*, 4th Int. Conf. on Earthquake Geotechnical Engineering—Conf., K. D. Pitilakis, ed., Springer, Netherlands.

Boulanger, R. W., and Idriss, I. M. (2014). "CPT and SPT based liquefaction triggering procedures." Rep. No. UCD/CGM-14/01, Center for Geotechnical Modeling, Dept. of Civil and Environmental Engineering, College of Engineering, Univ. of California, Davis, CA, 138.

Idriss, I. M., and Boulanger, R. W. (2008). "Soil liquefaction during earthquakes." Earthquake Engineering Research Institute, Oakland, CA, 261.

Arulanandan, K., Yogachandran, C., Meegoda, N. J., Ying, L., and Zhauji, S. (1986). "Comparison of the SPT, CPT, SV and electrical methods of evaluating earthquake induced liquefaction susceptibility in Ying Kou City during Haicheng Earthquake." *Proc., Use of In Situ Tests in Geotech. Engrg., Geotech. Spec. Publ. No.6*, ASCE, New York, N.Y., 389-415.

Ishihara, K., Acacio A. A., and Towhata, I. (1993). "Liquefaction-induced ground damage in Dagupan in the July 16, 1990 Luzon Earthquake." *Soils and Found.,* Tokyo, Japan, 33(1), 133-154.

Inthuorn Sasanakul, (2005), "Development of an electromagnetic and mechanical model for a resonant column and torsional shear," A dissertation submitted to Utah State University in partial fulfillment of the requirements for the degree of Doctor of Philosophy.

Sykora, D.W., and Stokoe, K.H., II, (1983), "Correlations of in situ measurements in sands with shear wave velocity," Geotechnical Engineering Report GR83-33, University of Texas at Austin, Austin, Texas.

Robertson, P.K., and Campanella, R.G., (1983), Interpretation of cone penetration tests – Part I: Sands," Canadian Geotechnical Journal, Vol. 20, No.4, pp. 718-733.

Rix, G.J., (1984), "Correlation of elastic moduli and cone penetration resistance," Thesis submitted to the University of Texas at Austin in partial fulfillment of the requirements for the degree of Master of Science.

Baldi, G., Bellotti, R., Ghionna, V., Jamiolkowski, M., and Pasqualini, E., (1986), "Interpretation of CPTs and CPTUs – Part II: Drained penetration in sands." *Proceedings,* Fourth International Geotechnical Seminar on Field Instrumentation and In Situ Measurements, Singapore.

Bellotti, R., Ghionna, V., Jamiolkowski, M., Lancellota, R., and Manfredini, G., (1986), "Deformation characteristics of cohesionless soils from in situ tests," Use of In Situ Tests in Geotechnical Engineering, Geotechnical Special Publication No. 6, S.P. Clemence, Ed., ASCE, pp. 47-73.

Lo Presti, D.C.F., and Lai, C., (1989), "Shear wave velocity from penetration tests," Atti del Dipartimento di Ingegneria Stutturale No. 21, Politecnico di Torino, Torino. Italy.

Baldi, G., Bellotti, R., Ghionna, V., Jamiolkowski, M., and Lo Presti, D.C.F., (1989), "Modulus of sands from CPTs and DMTs," *proceedings,* XII ICSMFE, Rio de Janeiro, Vol. 1, pp.165-170.

N. Janbu and K. Senneset. Effective Stress Interpretation of In Situ Static Cone Penetration Tests. *Proc*., 1st European Symposium on Penetration Testing, ESOPT I, Stockholm, Sweden, Vol. 2.2, 1974, pp. 181-195.

K. Senneset and N. Janbu, Shear Strength Parameters obtained from Static Cone Penetration Tests. In Strength Testing of Marine Sediments, ASTM STP 883, Philadelphia, Pa., 1985, pp.41-54.

Begemann, H. K., "Thte Friction Jacket Cone as an Aid in Determining the Soil Profile," Proceedings 6th International Conference on Soil Mechanics and Foundation Engineering, Vol. 1, 1965, pp. 17-20.

Sanglerate, G., Nhiem, T. V., Sejourne, M., and Andina, R., "Direct Soil Classification by Static Penetrometers with Special Friction Sleeve," Proceedings European Symposium on Penetration Testing, Stockholm, Vol. 2.2, June, 1974, pp. 337-344.

Sanglerat, G., The Penetrometer and Soil Exploration, Elsevier Publishing Company, New York, 1972.

Schmertmann, J. H., "Guidelines for Cone Penetration Test, Performance and Design," U.S. Department of Transportation, Federal Highway Administration Report No. FHWA-TS-78-209, 1978.

Bruce J. Douglas, A.M. ASCE, and Richard S. Olsen, M. ASCE, "Soil Classification using Electric Cone Penetrometer," October 1981.

Series: Alaska Park Science - Volume 13 Issue 2: Mineral and Energy Development https://www.nps.gov/articles/aps-v13-i2-c8.htm Long-term Risk of Tailings Dam Failure By David M. Chambers

Tailings dam spills at Mount Polley and Mariana by Judith Marshall, August 2018.

Report on the immediate causes of the failure of the Fundão Tailings Dam, by Norbert R. Morgenstern, Steven G. Vick, Cassio B. Viotti, and Bryan D. Watts. August, 2016.

West Virginia's Buffalo Creek Flood: A Study of the Hydrology and Engineering Geology, by William E. Davies, James F. Bailey, and Donovan B. Kelly in 1972. Geological Survey Circular 66.

Brazil dam disaster likely had same cause as previous one: official Gabriel stargardter feb 2019

Vick, S.G., 1983. Planning, Design, and Analysis of Tailings Dams. Wiley, New York.

Tailings Impoundment Failures: Are Geotechnical Engineers Listening? Geotechnical News, September, p. 31-36.

Review of the Kingston Fossil Plant Ash Spill Root Cause Study and Observations about Ash Management, Tennessee Valley Authority Office of the Inspector General, Tom D. Kilgore, July 23, 2009.

A Tidal Wave of Mud by Shasta Darlington, James Glanz, Manuela Andreoni, Matthew Bloch, Sergio Pecanha, Anjali Singhui and Troy Griggs, Feb. 9, 2019.